Western Graduate&PostdoctoralStudies

Western University
Scholarship@Western

Electronic Thesis and Dissertation Repository

10-16-2012 12:00 AM

Characterization of Solar Roadways Via Computational and Experimental Investigations

Rajesh Kanna Selvaraju
The University of Western Ontario

Supervisor
Dr. Samuel F. Asokanthan
The University of Western Ontario

Graduate Program in Mechanical and Materials Engineering
A thesis submitted in partial fulfillment of the requirements for the degree in Master of Engineering Science
© Rajesh Kanna Selvaraju 2012

Follow this and additional works at: https://ir.lib.uwo.ca/etd

 Part of the Applied Mechanics Commons, and the Energy Systems Commons

Recommended Citation

Selvaraju, Rajesh Kanna, "Characterization of Solar Roadways Via Computational and Experimental Investigations" (2012). *Electronic Thesis and Dissertation Repository*. 906.
https://ir.lib.uwo.ca/etd/906

This Dissertation/Thesis is brought to you for free and open access by Scholarship@Western. It has been accepted for inclusion in Electronic Thesis and Dissertation Repository by an authorized administrator of Scholarship@Western. For more information, please contact wlswadmin@uwo.ca.

CHARACTERIZATION OF SOLAR ROADWAYS VIA COMPUTATIONAL AND EXPERIMENTAL INVESTIGATIONS

(Spine title: Characterization of Solar Roadways)

(Thesis format: Monograph)

by

Rajesh Kanna Selvaraju

Graduate Program in Engineering
Department of Mechanical and Materials Engineering

A thesis submitted in partial fulfillment
of the requirements for the degree of
Master of Engineering Science

The School of Graduate and Postdoctoral Studies
The University of Western Ontario
London, Ontario, Canada

© Rajesh Kanna Selvaraju 2012

THE UNIVERSITY OF WESTERN ONTARIO
School of Graduate and Postdoctoral Studies

CERTIFICATE OF EXAMINATION

Supervisor

Dr. Samuel F. Asokanthan

Supervisory Committee

Dr. Anand V. Singh

Examiners

Dr. Liying Jiang

Dr. Rajiv K. Varma

Dr. Takashi Kuboki

The thesis by

Rajesh Kanna Selvaraju

entitled:

CHARACTERIZATION OF SOLAR ROADWAYS VIA COMPUTATIONAL AND EXPERIMENTAL INVESTIGATIONS

is accepted in partial fulfillment of the
requirements for the degree of
Master of Engineering Science

Date

Chair of the Thesis Examination Board

Abstract

Efficiency of traditional solar panels is known to be very low and hence necessitates the use of extensive open spaces for producing solar-based electric power. In solar roadways concept, open spaces such as roads, parking lots, bicycle lanes, footpaths are proposed to be utilized. An in-depth quantitative feasibility study for implementing solar roadways in Canada is carried out considering the total available surfaces, solar panel efficiency and effects of fast moving shades. The load carrying capability of commercially available materials for the solar panel top cover is studied in an effort to examine the current as well as near-future implementation of this proposed concept. In addition, a piezo-based auxiliary energy harvesting system is proposed for harnessing the vehicle-induced strain on the solar panel top cover. The positions of the piezoelectric elements are optimized by studying the vibration characteristics of the top cover via numerical as well as experimental methods.

Keywords:

Solar Roadways, fast moving shades, solar panel top cover, vibration characteristics, energy harvesting.

Acknowledgments

I would like to take this opportunity to acknowledge and thank those who have supported, encouraged, and guided me in this work.

I would first like to express my sincere gratitude for the guidance, advice, assistance, and support of my supervisor, Dr. Samuel F. Asokanthan, and the suggestions made by Dr. Anand V. Singh on my advisory committee. I would also like to thank my colleagues in the Dynamic and Sensing Systems Laboratory at UWO, from whom I have learned many things during my time there. I'd like to thank my parents and friends for their encouragement and support in my studies.

Funding for student support and experimentation in thesis was partially made available by the Ministry of Transportation, Ontario (MTO) under the grant scheme Highway Infrastructure Innovations Funding Program (HIIFP) which is also gratefully acknowledged.

Table of Contents

List of Tables

List of Figures

List of Appendices

NOMENCLATURE

D	Dielectric displacement
d	Piezoelectric charge constant
E	Electric field
G	Solar irradiance
H	Gross weight of two axle truck
HS	Gross weight of multi axle truck
$\mathbf{I}$	Intensity of the light transmitted through a layer of material
I	Output current from the solar cell
I_L	Photocurrent
$\mathbf{I_0}$	Intensity of the light incident on the material
I_o	Dark saturation current
I_M	Output current from the solar module
I_{sc}	Short circuit current
I_{scM}	Short circuit current of the solar module
$iscm$	Short circuit current of the solar module
ln	Natural Logarithm
n	Diode ideality factor
N_p	Number of solar cells in parallel

N_s	Number of solar cells in series
R_s	Series resistance
R_{sh}	Shunt resistance
R_{sM}	Series resistance of the solar module
S	Mechanical strain
s^E	Elastic constant
$\mathbf{T}$	Mechanical stress
T	Temperature
V	Voltage across the output terminal
V_M	Voltage across the output terminal of the solar module
V_{oc}	Open circuit voltage
V_{ocM}	Open circuit voltage of the solar module
V_T	Thermal voltage
x	Thickness of the material
α	Absorption coefficient
ε^T	Permittivity

ACRONYMS

AADT	Annual Average Daily Traffic
AASHTO	American Association of State Highways and Transportation
AC	Alternating Current
DAQ	Data Acquisition
DC	Direct Current
FFT	Fast Fourier Transform
LABVIEW	Laboratory Virtual Instrumentation Engineering Workbench
LVD	Lased Doppler Vibrometer
MIT	Massachusetts Institute of Technology
N/A	Not Applicable
OCAA	Ontario Clean Air Alliance
OPG	Ontario Power Generation
PSPICE	Personal computer Simulation Program with Integrated Circuit
PSV	Polytec Scanning Vibrometer
PZT	Lead Zirconate Titanate
STC	Standard Test Condition
VI	Voltage-Current product

Chapter 1

1 Introduction and Review of Literature

1.1 Motivation

Global warming has become one of the most complicated issues faced by the world in the present century, and has resulted in a drastic change in the climate all over the world in recent years. The climate change has been observed via the instrumental temperature record, rising sea levels, and decreased snow cover in the Northern Hemisphere. These undesirable changes may be attributed to the large amount of carbon dioxide released into the earth's atmosphere. The industrially developed nations are often made to take responsibility for these changes as they have been emitting the greenhouse gases without any restriction starting from the days of industrial revolution. Hence, Canada, in particular, the province of Ontario is recognized as one of the industrially advanced North American provinces, has a duty to protect the natural environment and to reduce the emission of greenhouse gases.

Increase in the use of renewable energy resources has been considered as one of the primary solutions to reduce the global warming. Different types of renewable energy resources such as solar, wind, ocean and geothermal energy resources are available abundantly. Among all these renewable energy resources, solar energy is the only resource available all over the world abundantly and distributed more evenly. Hence developing technologies to use this solar energy will be the most appropriate at these transition times.

In order to overcome the relatively low efficiency of the solar panels, significantly large amount of open spaces are required in the photovoltaic solar panel applications for the production of electricity to meet the present energy demands. However, availability of large open spaces is on the decline near the urban areas and hence the solar panels can only be installed in remote areas, which may result in huge energy losses while transporting electricity. The low efficiency of the solar panels as well as the necessity to deal with the transmission losses makes the use of solar panels a non-viable economical

option to produce electricity. In order to make the solar power a viable economical option, open spaces that are available closer to the highly populated (high energy demand) areas must be identified. Hence, it is proposed that open spaces such as the roads, parking lots, bicycle lanes, footpaths etc. be utilized for this purpose. In order to use these open spaces for producing electricity using solar panels, recently, the concept of solar roadways have been introduced. The concept of solar roads has now emerged as a strong contender where the solar energy collectors can be incorporated directly in the design of highway infrastructure and the energy can be transferred directly through the available grids or sent to storage facilities for later use. Thus, the primary objective of this research is to investigate the feasibility of this novel idea keeping in mind the long term sustainability while giving importance to safety and performance. In an effort to ascertain the feasibility, the present study will consider important factors such as roadway surface material durability/performance, solar panel efficiency and various losses involved in this system as well as ways to overcome them. At present, the solar road project is primarily being spearheaded by a US-based company 'Solar Roadways Inc.' [1] in association with some academic institutions.

There are many advantages in following up the development of this technology which is expected to yield major contribution to the current global energy requirement. Hence, by using solar roadways, huge amount of carbon dioxide produced by the power plants can be reduced to a considerable level which can prevent global warming. Also, the dependence on nuclear power plants can be reduced and the nuclear disasters like the one recently occurred in Japan can be avoided. The electric vehicles produced now by various automobile manufacturers are meant for short range i.e. they can only travel up to few hundred kilometers after which the batteries need recharging. With solar roadways, road side charging stations can be developed so that the electric cars can be recharged. Thus, the dependence on gasoline can be reduced and hence the contribution to the greenhouse effect by automobiles can be reduced. The solar roadways technology can also help the countries whose economy is largely affected by the price rise of oil. This technology can also lead to the development of ultra-modern intelligent highway systems which consists of LEDs for painting the road lanes from beneath the surface in order to make the roads visible during the worst driving conditions. Further use of this power can be utilized in

developing temperature sensitive heating elements to prevent snow/ice accumulation during the extreme winter climates, and microprocessor boards for control and communications. With this form of arrangement, the potential applications are numerous, and should this technology matures, these forms of possibilities would be endless.

One of the primary limitations in employing this technology is in finding a suitable material that can substitute the glass cover on the solar panels. This material must have the desirable properties to withstand the load of vehicles moving over the panel while providing sufficient traction between the road surface and the wheels. Hence, a study is required for investigating the load carrying capability of the commercially available materials for the solar panel top cover. This study needs to be based on the stress as well as the deflection analysis, and a platform when developed may aid further development of a suitable panel cover for this application. The specific losses that are involved in this technology such as the fast moving shade effect due to the vehicles moving over the solar panels must also be identified and the effects must be addressed in the analysis. Other environmental and technical factors such as solar cell temperature and uncertainty in solar irradiation that can influence the solar panel output also need attention in an effort to understand the effects on overall power output. In order that this technology can be implemented in the near future, it is desirable that an auxiliary energy harvesting system be developed for this application. The need for such a system is seen in additional power production for compensating the various energy losses associated with the solar panel.

1.2 **Literature Review**

1.2.1 Requirement for alternative energy resources

Ontario Power Generation (OPG) has five thermal power stations with a total power generation capacity of 5447 megawatts [2]. The fuels for the thermal power plants in Canada are coal, oil or natural gas. According to the Ontario Clean Air Alliance (OCAA) report, thermal power plants in Ontario are the major source for polluting environment. OPG's coal power plants produce 40 percent of the total carbon dioxide emissions in Ontario [3]. In order to reduce the environmental pollution, OPG is making an effort to

phase out the coal fuelled power plants in the near future. Thus, there is a need to find an alternate source of energy for electricity production.

1.2.2 Fast moving shade effects on solar panel

Solar panels have an average efficiency between 15 to 17 percent, when operating under standard test condition (STC) with solar irradiance of 1000 w/m^2, air mass coefficient of 1.5 and the cell operating temperature of 25° C [4]. For many years, studies have been conducted to improve the efficiency of the solar panels to convert the sunlight falling on them into electricity. One of the main causes for the drop in the electricity produced by the solar panels is the shade that falls over a solar panel. The effects of shade over the solar panels have been studied through both software and experimental simulations. The effects of non-uniform solar irradiance distribution on output of the solar panel array have been studied by Engin et al. [5] and they proposed a model to analyze the photovoltaic array with sufficient degree of precision and also demonstrated that the proposed model does not increase the computational effort, when the size of the photovoltaic array analyzed are increased. Achim et al. [6] have studied the effects of partial shading on photovoltaic arrays and have identified that partial shading is one of the main causes for reduction in the energy generated by the grid connected photovoltaic systems. M.C. Alonso et al. [7] have simulated the shade effect in arrays with different cell configuration and proposed the best configuration to minimize the effects of partial shading. L. Cortez et al. [8] have studied the effects of random changes of solar radiation on the energy generated by the solar panels. Ramaprabha [9] has simulated the effect of partial shading on a series and parallel connected solar photovoltaic module using PSPICE and concluded that the effects of partial shading on the photovoltaic cells of a parallel connected photovoltaic module is less when compared to that of a series connected module. It may be noted that all of the above studies performed on the effects of partial shading over the photovoltaic arrays have identified partial shadowing as one of the main causes for the reduction in the energy generated by the photovoltaic systems.

Shade effects on solar panel considered in the above studies are primarily attributed to the obstructions caused by buildings or trees when the sun light falls over the solar panels. These shades are always found to be dependent on the position of the sun and hence the

effects of these shades remain for a sufficiently long period. Another type of shade effect already studied for the solar panels are the shades caused due to stains over the solar panels by the collection of dust [10] or due to the collection of snow over the solar panels. The above studies provide some insight into the methods and models that can be used for the present study to be carried out on the Solar Roadways application. However, in the present application, the shade effects due to vehicles moving over the panel is considered to play a more significant role and hence given more prominent attention. This class of shades can be considered as 'fast-moving' as opposed to the shades studied in the previous studies are that 'slow-moving'. The present study on the solar roadways application hence focuses on the former knowing that the effects due to the latter can always be added when there is a need for inclusion.

1.2.3 Material for the solar panel top cover

One of the main problems in implementing the solar roadways system is in the material selection for the top cover of the solar panel. It is quite obvious that the material selected for the top cover must possess sufficient structural strength to take on the vehicle load moving over it while possessing surface properties similar to those of roads, so that the vehicles moving over it will have sufficient traction to move and stop safely in slippery conditions like rain and snow. Scott Brusaw of Solar Roadways attempted to partner with the researchers at the Pennsylvania State University's Materials Research Institute to develop a glass that can be used as a top cover for the solar panels of solar roadways application [11]. As part of this study, Material scientist John Hellmann of Pennsylvania State has stated that glasses can theoretically be made to have a very high strength, provided that they are manufactured with extremely reduced flaws. At present, glasses are being made available for many structural applications following this approach. Further, Richard Brow of Missouri University of Science and Technology states that the glass can be strengthened by compressing its surface using special heating technique or at a molecular level. These glasses are found to be ten times stronger than the normal glasses [11]. Since this material technology is at its infancy, for solar roadways application, commercially available materials and their ability to take on the load of vehicles moving over a typical panel cover is analyzed first in an effort to develop a

simulation platform that can be used when such a material becomes available commercially.

1.2.4 Piezoelectric energy harvesting system

Energy harvesting is a process that absorbs small amount of energy that would otherwise go as waste in the form of heat, light, sound, vibration or movement and converts them into a useful form of energy [12]. Energy harvesting methods are mostly employed for improving the efficiency of the system. Piezoelectric materials are a type of energy harvesting materials. In the recent past, significant research efforts have gone into studying the use of piezoelectric materials for absorbing the mechanical energy and converting into electrical energy. Recently, two MIT students demonstrated that the piezoelectric material can be implanted in the floors where more people walk over and that the force generated by people walking over these floors can be harnessed to produce electricity. This energy harvesting system has been used in the dance floors of the clubs, where 5 to 10 watts of electricity is generated by an individual dancing on the floor [13]. East Japan Railway Company conducted an experiment to produce electricity by installing piezoelectric elements in the floors of its Tokyo station, where people pass through the gates. They extracted an output of 1400 KW per second by covering an area of 25 square meters [14]. Innowattech energy harvesting systems developed a technology to convert the mechanical energy of the vehicles passing over the road into electrical energy by laying piezoelectric elements below the asphalt surface of the roads [15]. Hence, this form of piezoelectric energy harvesting system appears to be a promising contender for the solar roadways application. In the present study, such an attempt will be made to harness the strain energy produced at the solar panel top cover support interface to produce electricity.

1.3 Thesis Aims and Outline

1.3.1 Thesis Aims

The research described in this thesis is directed towards implementation of solar roads and investigation of the associated challenges. For the purposes of achieving this objective, the following steps have been considered:

- A detailed analysis on the feasibility of implementing solar roadways concept in Canada is to be carried out. The primary purpose of this study is to provide quantification of the amount of electricity that can be generated by covering the total available road surfaces with solar panels. The predictions are to be then compared with the current electricity demand for Canada.

- The effect of fast moving shades over the solar panels of solar roadways system and various other losses are to be studied via simulation. PSpice software is selected for this purpose and conditions these solar panels are subjected to in real life are to be included in the simulation study. For simulation purposes, various vehicles such as tractor semi-trailer, full size car and intercity bus moving over the solar panel are to be considered. These simulation results need to be validated in the laboratory employing commercially available solar panels. For this purpose and for future experimentation in this area, a LabVIEW based data acquisition system is to be developed.

- The load carrying capability of the commercially available materials for the solar panel top cover is to be studied numerically. COMSOL Mulitphysics software to conduct this numerical study together with the possibility of predicting the required material properties are to be examined. It is proposed that the weight of a truck, a car and a motorbike be used in the analysis as important case studies. This study is envisaged to aid investigation of the feasibility of material to be developed for the solar panel top cover in the near future.

- Investigation of a piezoelectric based auxiliary energy harvesting system is to be conducted for the purpose of harnessing the strain energy available at the solar panel top cover support interface. The strain is expected to be generated from the vehicles moving over the top cover. A procedure for optimizing the locations of piezoelectric elements in the solar panel to increase the efficiency of the energy harvesting system is to be developed via COMSOL Mulitphysics software as well as vibration experiments.

1.3.2 Thesis Outline

In the present chapter, the research which will be presented in the following chapters has been introduced and relevant literature is reviewed. In chapter 2, a detailed discussion on the feasibility study for the Solar Roadways application in Canada is presented. This analysis is performed by calculating the amount of electricity that can be generated by covering all the road surfaces with solar panels and comparing it with the electricity demand for Canada. The effects of fast moving shades on the solar panels studied via simulation are documented and discussed in Chapter 3. The numerical results obtained via PSpice software for various vehicular cases have been validated experimentally in the laboratory considering a typical shade moving over a solar panel array built from commercially available solar panels. Other factors which affect the efficiency of the solar panels are also discussed in this chapter. In chapter 4, a typical commercially available material that can be used for building solar panels for the solar roadways application is studied. The difference between the maximum load taken by this material and the maximum load that needs to be taken up by future solar panels for solar roadways application is compared using the COMSOL Multiphysics software. A procedure to systematically perform a preliminary analysis of any material to be developed for the solar panel top cover is also developed. In Chapter 5, a piezoelectric based auxiliary energy harvesting system to harness the strain energy due to vehicles moving over the solar is investigated. A procedure for optimizing the locations of piezoelectric elements in the solar panel to increase the efficiency of the energy harvesting system is developed via COMSOL Mulitphysics software as well as vibration experiments. In Chapter 6, the main results of this thesis are summarized and topics for future research are identified.

Chapter 2

2 Feasibility study for Canada

2.1 Introduction

In this chapter, an analysis for predicting the feasibility of implementing Solar Roadways in Canada is carried out. This analysis primarily provides quantification of the amount of electricity that can be generated if the total available road surfaces are covered with solar panels, while comparing the total possible energy output with the current electricity demand for Canada. The discussion also gives an insight into province-wide solar roadways energy availability break-down. Further, the predictions assume the use of the most efficient solar panel that is available in the market while considering mean daily global insolation data for each province.

2.2 Length of Roads

Total length of roads available in each province of Canada is calculated using the data taken from the Applied Research Associates report submitted to Transport Canada [16]. This data gives a reasonable estimate on the total area of open spaces that are readily available in Canada for the Solar Roadways application. In order to find the total length of available roads, freeways, arterial roads, collector roads and local roads under federal, provincial and municipal jurisdiction levels are taken into consideration. It is worth mentioning that in addition to these available roads, open spaces such as parking lots, rooftops, foot paths, cycle paths and bridges which are readily available in the vicinity of places where people live can be covered with solar panels, so that the losses due to the long distance transmission of the electricity can be reduced. As there are not enough data available on these open spaces, only the roads are taken into consideration for the present predictions. Total length of roads available in each province of Canada is shown in Table 2-1.

Table 2-1 Lengths of roads in each province of Canada

Province	**Total length of roads available in each Province (km) - Two lane equivalent**
Alberta	56240.5
British Columbia	12516
Manitoba	18693
New Brunswick	18027.6
Newfoundland & Labrador	9721.5
North western territories	2183
Nova Scotia	25239.6
Nunavut	N/A
Ontario	19661
Prince Edward Island	40.7
Quebec	89706
Saskatchewan	198691
Yukon	4788
Total	455507.9

It may be noted that in the data provided in Table 2-1, municipal road details for the Newfoundland & Labrador, Prince Edward Island, New Brunswick, Ontario, Manitoba and British Columbia provinces are not found in this report [16]. Further, as indicated in the table, details of Nunavut province were also not found in this report and hence not considered in the analysis. However, for the province of Ontario in addition to the length provided in Table 2-1, the total length of the available municipal roads is taken as 51770 km based on the data provided in the 2003 Ontario Municipal Roads report [17]. The average widths of roads in Canada based on the Road Rehabilitation Energy Reduction Guide for Canadian Road Builders report [18] are considered as 3.67 m (12 feet). Based

on the above data, the total area in the form of roads available for conversion into Solar Roadways is estimated to be 3522 km^2.

2.3 **Selection of solar panel**

Solar panels for the calculation purpose are selected based on their efficiency to convert the sunlight falling on them into electricity. According to The Windsor Square news report, the most efficient solar panel available in the Ontario market at present are the solar panel manufactured by Windsor's Unconquered Sun solar technologies which has an efficiency of 16.0% [19]. Thus Windsor 250^{TM} poly solar panel is selected for the present calculations. The specifications for the Windsor 250^{TM} poly solar panel at standard test conditions [20] is given in Table 2-2. The specification for the solar panel is based on the standard test conditions (STC) of solar irradiance 1000 w/m^2, air mass 1.5 and the cell operating temperature of 25° Celsius [4].

Table 2-2 Specification of the Windsor 250^{TM} solar panel

Maximum Power	250W
Tolerance of Maximum Power	± 5%
Open circuit voltage	37.2V
Maximum Power voltage	30.1V
Short circuit current	8.87A
Maximum Power current	8.30A
Module Efficiency	16.0%
Type of cells	Polycrystalline silicon
Cell configurations	60 in series
Dimensions (Length x Breadth x Height)	1644mm x 972mm x 50mm

2.4 **Mean daily global insolation**

Insolation (also known as solar irradiation) is a measure of the solar radiation received by a given area over a given period of time [21]. The unit used for insolation is either MJ/m^2 or kWh/m^2. The mean daily global insolation will give a measure of total solar energy available in each province of Canada. In order to calculate the amount of electricity that can be produced by the solar panels, the solar insolation data for each province are required, so that the calculated amounts of electricity that can be produced by the solar panels are closer to the actual electricity that will be produced under real environmental conditions. The mean daily global insolation values given in Table 2-3 for each province are obtained from the photovoltaic maps published by Natural Resources Canada [22] shown in Figure 2-1.

For the purpose of evaluating the mean daily global insolation, the following factors have been taken into consideration:

- Solar panel orientation is treated as horizontal for this case, as they are going to be placed on roads.
- Period for which the mean daily global insolation is considered is annual. This consideration is made as we require data for calculation purposes only. The period can also be considered on a monthly or daily basis instead of annual, for more accurate calculations.
- Maximum and minimum available mean daily global insolation value as depicted in Table 2-3 are taken into consideration, so that an upper and lower bound estimate of the amount of electricity that may be produced by the Solar Roadways system can be predicted.

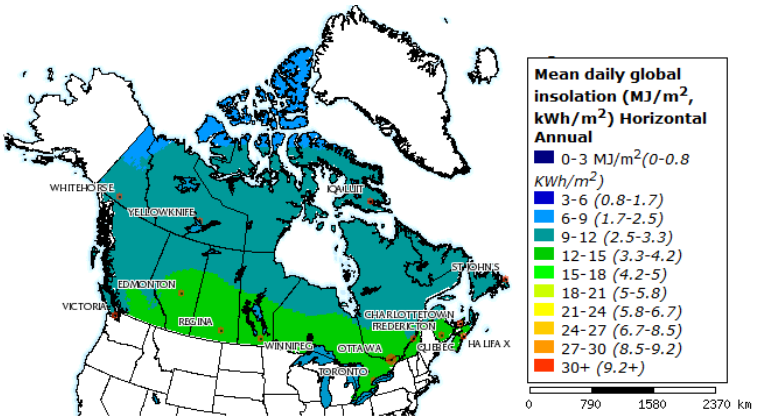

Figure 2-1 Mean daily global insolation map for Canada taken from Natural Resources Canada

Table 2-3 Mean Daily Insolation Data for each province in Canada

Province	**Mean Daily Insolation (kWh/m^2)**	
	Minimum	**Maximum**
Alberta	3.3	4.2
British Columbia	2.5	3.3
Manitoba	3.3	4.2
New Brunswick	3.3	4.2
Newfoundland and Labrador	2.5	3.3
North western territories	2.5	3.3
Nova Scotia	3.3	4.2
Nunavut	2.5	3.3
Ontario	3.3	4.2
Prince Edward Island	2.5	3.3
Québec	2.5	3.3
Saskatchewan	3.3	4.2
Yukon	2.5	3.3

2.5 **Energy produced in each province based on selected parameters**

Based on the available length and width of road for each province, total area available for converting into Solar Roadways is calculated. Then based on the average daily sun peak hours (i.e. number of hours in a day a location will have solar irradiation of 1000 watts per square meter), total sun peak hours available for a year in each province is calculated. Finally, based on the calculated area, total yearly sun peak hours in each province and using the data form the selected solar panel, the energy that can be produced in each province by solar roadways is calculated and shown in Table 2-4.

Thus a total of 7.98×10^5 GW-hour of energy per year can be produced in Canada, by covering all the roads available with the solar panels based on the maximum yearly insolation value, while an amount of 6.23×10^5 GW-hour of energy per year based on the minimum yearly insolation value. Known that the electricity usage in Toronto is 25000 GW-hour of energy per year [23], it may be estimated that Solar Roadways if implemented in Canada will be able to supply power to maximum of 32 or minimum of 25 cities similar in size to Toronto.

Figures 2-2 and 2-3 show the total area available as roads in each province and the energy produced by covering all these roads with solar panels. These figures show that the provinces Saskatchewan, Québec, Alberta and Ontario are the top four provinces which can benefit maximum from the Solar roadways system.

Table 2-4 Total energy produced from Solar Roadways in Canada

Province	**Total Road Length (km)**	**Total Area (km^2)**	**Yearly insolation ($kWhr/m^2$)**		**Total energy produced (kWhr)**	
			Max.	**Min.**	**Max.**	**Min.**
Alberta	112481	411.41	1533	1204.5	9.85×10^{10}	7.74×10^{10}
British Columbia	25032	91.56	1204.5	912.5	1.72×10^{10}	1.30×10^{10}
Manitoba	37386	136.74	1533	1204.5	3.27×10^{10}	2.57×10^{10}
New Brunswick	36055.2	131.88	1533	1204.5	3.16×10^{10}	2.48×10^{10}
Newfoundland and Labrador	19443	71.11	1204.5	912.5	1.34×10^{10}	1.01×10^{10}
North western territories	4366	15.97	1204.5	912.5	3.00×10^{09}	2.27×10^{09}
Nova Scotia	50479.2	184.63	1533	1204.5	4.42×10^{10}	3.47×10^{10}
Nunavut	N/A	N/A	1204.5	912.5	N/A	N/A
Ontario	91092	333.18	1533	1204.5	7.97×10^{10}	6.27×10^{10}
Prince Edward Island	81.4	0.30	1204.5	912.5	5.60×10^{07}	4.24×10^{07}
Québec	179412	656.22	1204.5	912.5	1.23×10^{11}	9.35×10^{10}
Saskatchewan	397382	1453.46	1533	1204.5	3.48×10^{11}	2.73×10^{11}
Yukon	9576	35.03	1204.5	912.5	6.59×10^{09}	4.99×10^{09}
Total	962785.8	3521.5			7.98×10^{11}	6.23×10^{11}

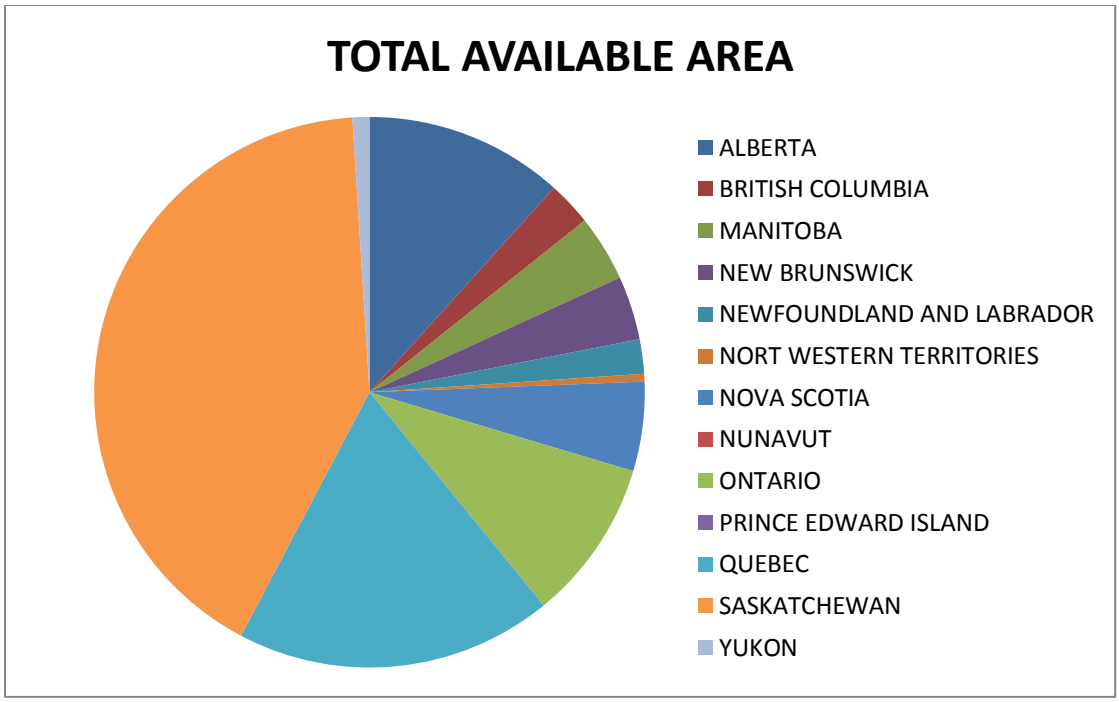

Figure 2-2 Total area available as roads in each province to be covered by solar panels

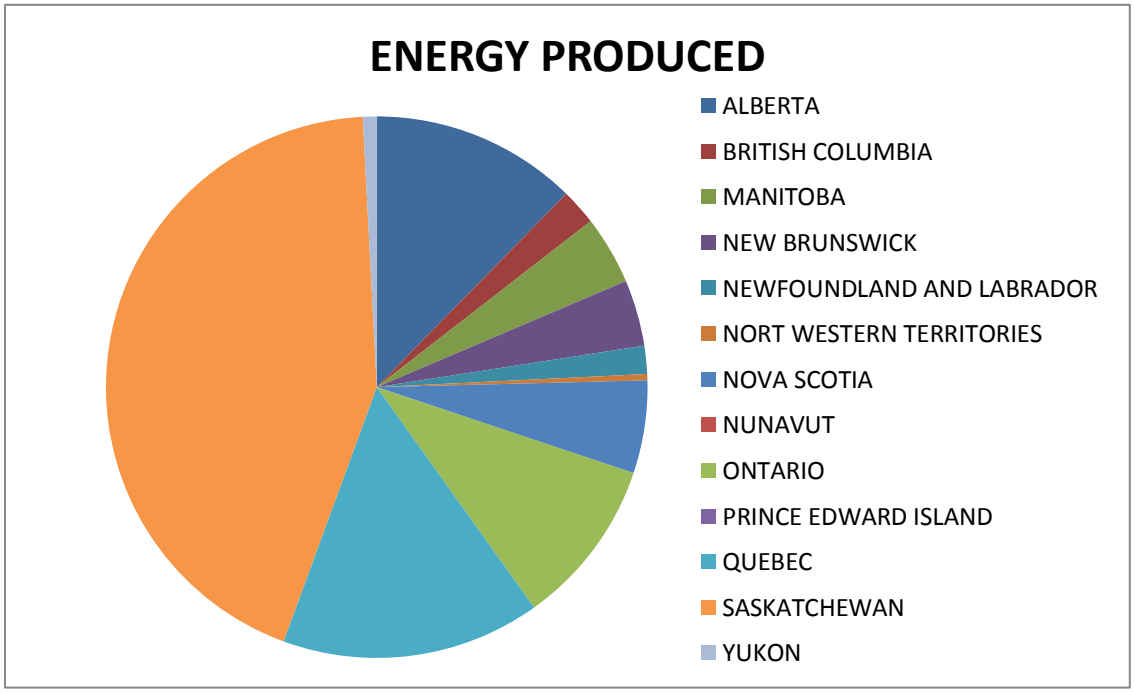

Figure 2-3 Energy produced in each province by the Solar Roadways system

2.6 **Summary**

In this chapter, a feasibility study for a Solar Roadways system in Canada has been conducted by calculating the total area available in the forms of roads and total amount of electricity that can be generated by covering these open spaces with solar panels. Based on the maximum and minimum values of available insolation, energy produced in each province has been calculated. It is clear that the electricity generated just by covering all the roads in Canada with the solar panels, would be sufficient to meet the power demands of 32 cities similar in size to Toronto. Saskatchewan, Québec, Alberta and Ontario are the top four provinces which can benefit maximum from the Solar roadways system.

Chapter 3

3 Power output variation due to panel and environmental influence

3.1 Introduction

The effect of shades on solar panels has been studied through software or experimental simulations in the recent past in an effort to maximize solar panel output. However, the shade effects on solar panel considered have been limited to the obstructions caused by buildings or trees to the sun light falling over the solar panels. These types of shades always depend on the position of the sun. The effect caused by these shades remains for a very longer duration and hence considered to be quasi-static in nature. The effects caused by the shade on the electricity production of solar panels will be present for hours to days. Shading over 5% of the area of the solar panel can reduce output power to as low as 50% [24]. However, in Solar Roadways application, in addition to the cases studied above, vehicles moving over the solar panels cause fast moving shades to appear over the panels. Typically it is expected that the effect of these shades on the electricity production by solar panels will be present for only a few seconds depending on the speed of the vehicle moving over it. Hence in solar roadways application it is necessary to study the effect of this form of shades. In the present study, PSpice software has been employed to simulate the effects of fast moving shadows on the solar panels and these results are justified by simulating the similar conditions experimentally.

3.2 PSpice

The name PSpice is an acronym Personal computer Simulation Program with Integrated Circuit Emphasis. Spice was originally an open source electronic analog circuit simulator, developed at the University of California [25]. PSpice has been developed from Spice and it can be used for both analog and digital circuit simulation. In the present study, a popular version of this software Cadence PSpice A/D has been employed. In this software, programs which symbolize the equivalent electrical circuit of the solar panel are synthesized and their outputs have been studied for various typical inputs. Thus these programs can be used to simulate the response of solar panel output,

without the need of building the complete real electrical circuits. In this analysis, equivalent electrical circuit of the solar panels are modeled using the simple current source, voltage source, diodes and resistors that are available in the PSpice library and the effect of shades on the output of the solar panels have been quantified.

3.3 **Equivalent electrical circuit of the solar panels**

Equivalent electrical circuit for the solar panels [26] is shown in Figure 3-1. The solar irradiance received by the solar cells is given as an input current to a voltage controlled current source. This is based on the equation

$$I_L = \frac{iscm}{1000} G \quad , \qquad 3\text{-}1$$

where I_L represents the photocurrent, G denotes the solar irradiance in W/m^2, and $iscm$ the short circuit current of the solar module measured under a standard test condition [4]. (The standard test conditions for the solar panels are solar irradiance value of 1000 W/m^2 and the solar cell temperature of 25°C and an air mass coefficient of 1.5)

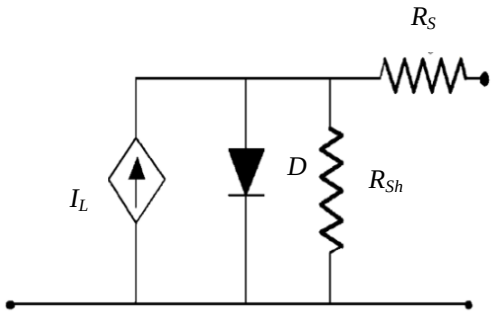

Figure 3-1 Equivalent electrical circuit model for solar panels

In the equivalent electrical circuit model for the solar panels shown in Figure 3-1, a series resistor R_S, shunt resistor R_{Sh} and diode D are also included. The series resistor included in the model represents the series resistive losses which are present in the actual solar panels. These losses are caused primarily due to the movement of current generated by the solar cells through the emitter and base of the solar cells and partly due to the contact resistances [27]. A series resistive loss reduces the fill factor (Fill factor is the ratio of actual maximum obtainable power to the product of open circuit voltage and short circuit

current) and the short circuit current of the solar cells. In order to include shunt resistive losses which are present in the actual solar panels, a shunt resistor has been included in the model. It may be noted that shunt resistance is also referred to as parallel resistance. Shunt resistive losses are caused in the solar cells primarily due to manufacturing defects present in the solar cells. Shunt resistive losses are also known to be larger when the sunlight falling over the solar cells are at low levels. In practice, it has been realized that it is difficult to produce an ideal IV characteristic in this class of devices. In order to overcome this, a diode is included in the equivalent electrical circuit model. Thus, the IV characteristics of the equivalent electrical circuit of the solar panel is based on the equation

$$I = I_L - I_0 \left(e^{\frac{V+IR_S}{nV_T}} - 1 \right) - \frac{V+IR_S}{R_{Sh}} \quad , \qquad 3\text{-}2$$

where I is the output current from the solar cell, I_0 is the dark saturation current (i.e. diode leakage current density in the absence of sunlight [27]), V is the voltage across the output terminal, R_S and R_{Sh} are the series and shunt resistance respectively, n is the diode ideality factor which is a number between 1 and 2 and V_T is the thermal voltage depending upon the absolute temperature T in kelvin.

Short circuit current for the equivalent electrical circuit model of the solar panel is given by substituting $V = 0$ (i.e. the output voltage is being set to zero) in the IV characteristic equation 3-2:

$$I_{sc} = I_L - I_0 \left(e^{\frac{I_{sc}R_S}{nV_T}} - 1 \right) - \frac{I_{sc}R_S}{R_{Sh}} \quad , \qquad 3\text{-}3$$

where I_{sc} is short circuit current of the solar panel.

Open circuit voltage for the equivalent electrical circuit of the solar panel is obtained by substituting $I = 0$ (i.e. the output voltage is set to zero) in the IV characteristic equation 3-2. It is known that the open circuit voltage is independent of the series resistance value and also the shunt resistance value [26]. Hence those terms involving the series and

shunt resistance value in the IV characteristic equation 3-2 can be neglected, to obtain the expression for the open circuit voltage V_{oc}:

$$V_{oc} = nV_T ln\left(1 + \frac{I_L}{I_0}\right) \quad . \qquad 3\text{-}4$$

In a typical solar panel, several solar cells are connected in series and parallel. In order to model a solar panel into an equivalent electrical circuit, some assumptions have to be made. The shunt resistances of the solar cells are assumed to be larger, so that its effects can be neglected, and the photo generated current I_L is assumed to be equal to that of the short circuit current I_{sc} of the solar cell [26]. The scaling rule for a solar panel where the number of cells in series is N_s and number of cells in parallel is N_p results in:

$$I_M = N_P I \quad , \quad I_{scM} = N_P I_{sc} \quad , \qquad 3\text{-}5a$$

$$V_M = N_s V \quad , \quad V_{ocM} = N_s V_{oc} \quad , \qquad 3\text{-}5b$$

$$R_{sM} = \frac{N_S}{N_P} R_S \quad , \qquad 3\text{-}5c$$

where the subscript *M* stands for the solar panel module and while variable without the subscript *M* represents the parameter associated with a single solar cell.

3.4 **Selection of solar panel for PSpice model**

Parameters associated with Kyocera solar panels are obtained from the manufacturer specifications and are employed for synthesizing the PSpice equivalent electrical circuit model. Kyocera is considered as one of the early solar panel manufactures and commenced their research in solar energy back in 1975. They have developed one of the most efficient and cost effective solar panels available at present market. For both PSpice simulation and experimental comparison of results, Kyocera KD135SX-UPU solar panel was used. These panels are made of crystalline silicon solar cells. These cells are permanently encapsulated between a tempered glass cover plate and a back sheet which is secured in an aluminum frame [28]. Specifications of the Kyocera KD135SX-UPU solar panel under standard test conditions are given in Table 3-1.

Table 3-1 Specifications of Kyocera KD135SX-UPU solar panel

Maximum Power (P_{max})	135 W
Tolerance of Maximum Power	± 5%
Open circuit voltage (V_{oc})	22.1 V
Maximum Power voltage	17.7 V
Short circuit current (I_{sc})	8.37 A
Maximum Power current	7.63 A
Dimensions (Length x Breadth x Height)	1500mm x 668mm x 46mm

3.5 **Verification of solar panels power and IV specification via PSpice analysis**

In the equivalent circuit modeled for the solar panel in PSpice, shunt resistance is neglected and diode ideality factor is considered to be unity. The results from the simulation in PSpice has been used to verify the tested specification of the selected solar panel given in Table 3-1. The Voltage – Current (VI) characteristic curve and the power curve generated in PSpice are shown in Figures 3-2 and 3-3 respectively. In voltage – current (VI) characteristic curve the open circuit voltage is the voltage obtained when the current in the circuit is zero and the short circuit current is the current obtained when voltage in the circuit is zero. The peak value in the power vs. voltage curve gives the maximum power. The open circuit voltage, short circuit current and maximum power obtained from the figures is 22.47V, 8.37A and 136.8W respectively and conforms to the solar panel specification given in Table 3-1. This demonstrates that the properties of equivalent electrical circuit model for solar panel in PSpice and the actual solar panel match closely with an error of about 1 to 2%.

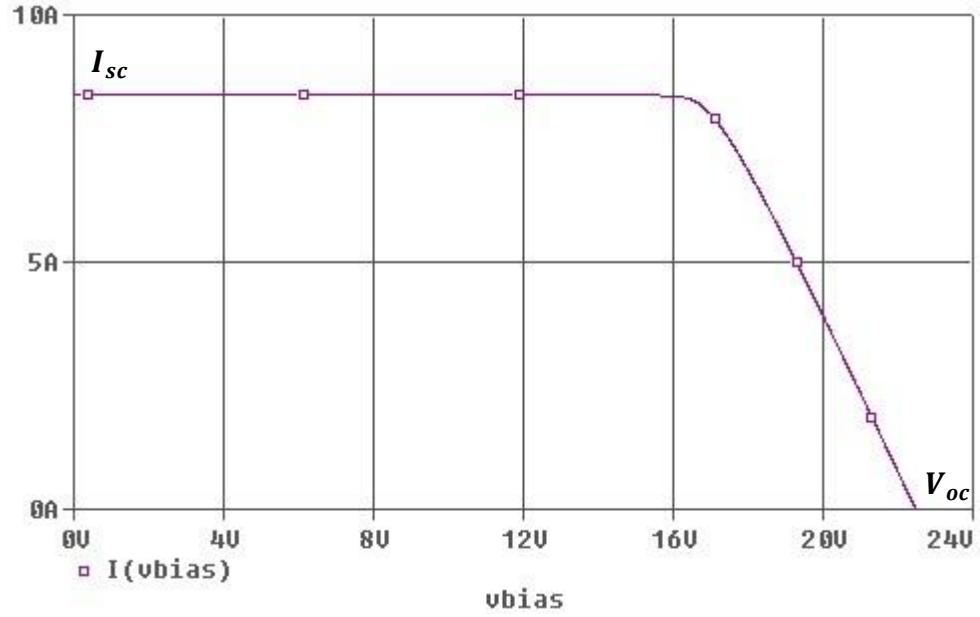

Figure 3-2 VI characteristic curve from PSpice analysis of the selected Kyocera KD135SX-UPU solar panel

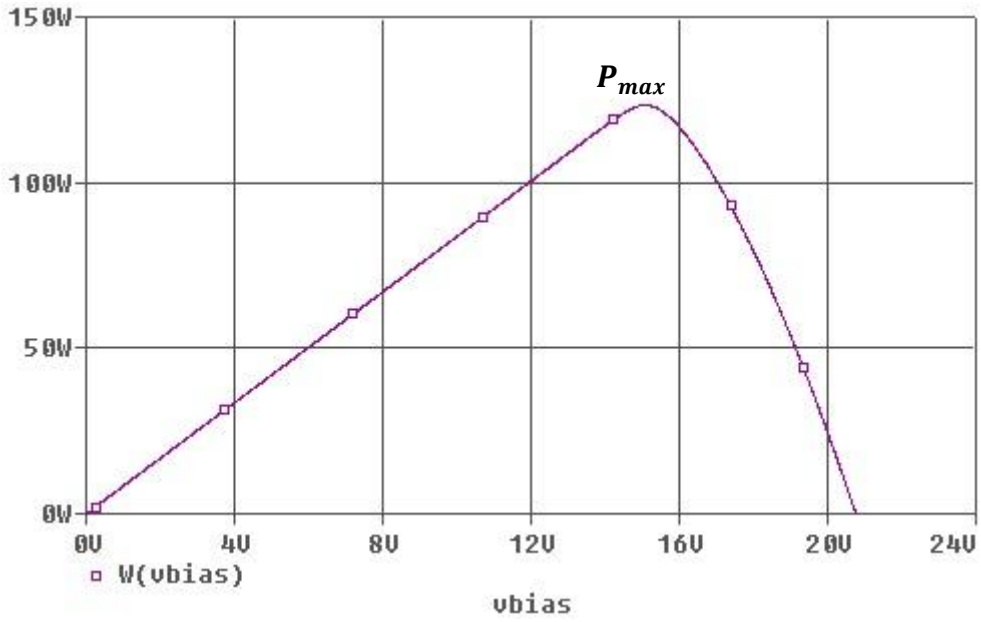

Figure 3-3 Power vs. Voltage curve from PSpice analysis of the selected Kyocera KD135SX-UPU solar panel

3.6 **Shade effect analysis**

In analyzing the effects of shades caused by the vehicles moving over the solar panels, the speed of the vehicle and the length of the vehicle are the two most important factors to be considered for calculating the time for which the shade will be present over the solar panels. In the present analysis, three types of vehicles are considered namely, a tractor semi-trailer, an intercity bus and a full size car. All three types of vehicles are considered to be travelling at a steady speed of 13.889 m/s (50 Km/hr). At the beginning of the simulation the solar irradiance is considered to be at 1 KW/m^2 which is the standard test condition parameter. As the vehicle starts to move over the solar panels, area of the solar panel covered with shade will increase and when the solar panel is fully covered by the vehicle, solar irradiance received by the solar cells is considered to reach a value close to zero. The solar irradiance value remains at zero for a few seconds as the length of the vehicle is larger than the length of the solar panel considered for the analysis. It is expected that condition will cause a sudden drop in power output from the solar panel. When the vehicle starts to move away from the solar panel, area of the solar panel covered with shade is expected to decrease and corresponding solar irradiance value received by the solar cells is expected to increase and to reach the value of 1 KW/m^2. When the vehicle completely moves away from the solar panel, the power output from the solar panels is expected to increase and to reach its full output level.

3.6.1 Time calculation

Based on the speed and length of the vehicle travelling over the solar panel, time taken by the vehicle to cross over the solar panel is calculated. For all of the time calculations, the length of the solar panel is considered as 1500 mm. when speed at which the vehicle moves over the solar panel is considered as 13.889 m/s (50 km/h), the time taken by the vehicle to move over solar panel can be calculated and are tested in Table 3-2.

Table 3-2 Time taken by the vehicles to cross over solar panel

	Tractor semi-trailer	**Intercity bus**	**Full size car**
Speed	13.889 m/s	13.889 m/s	13.889 m/s
Vehicle length	23 m	14m	4.9m
Total time to cross solar panel	1.77 sec	1.126 sec	0.471 sec
Time for complete solar panel cover	0.11sec	0.11sec	0.11sec
Time duration for complete solar panel cover	1.534 sec	0.890 sec	0.235 sec

3.6.2 Results from PSpice

In the present study on the shade effect caused by vehicles moving over the solar panels, analysis is performed between 0 to 10 seconds and at the 6^{th} second of the analysis the vehicle starts to pass over the solar panels. At this instant, the output terminal voltage of solar panels is at 35 volts and this condition is taken as a general consideration for all the cases. Also when the solar panels are fully covered by the shade, the amount of sunlight falling on the solar panels is taken as zero. Further to study the effect on multiple panels, two solar panels each with an output of 135W are connected in series. At any given instant only one panel is covered by the moving shade while the other panel receives full sunlight. It may be noted that in practice the shade may not cover the solar panels fully and the sunlight level may not exactly reach zero. However for analysis purpose these simplifications are made. As expected, the PSpice simulations show that the shade caused by a vehicle passing over the solar panel, will cause a sudden drop and rise in the power output from the solar panel as depicted in Figures 3-4 to 3-6. This sudden drop

and rise in the power output, depends mainly on the speed and length of the vehicle. As the speed of the vehicle increases the time duration between the drop and rise of the power output will start to decrease. Similarly, as the length of the vehicle increases, the time duration between the drop and rise of the power output will start to increase. It is worth pointing out for the solar roadways application, the system that is required to connect the power produced by the solar panels to the grid, must be capable to work with these rapid fluctuations in the power due to fast moving shades. The simulation study presented in this study provides an insight into the required power conditioner design.

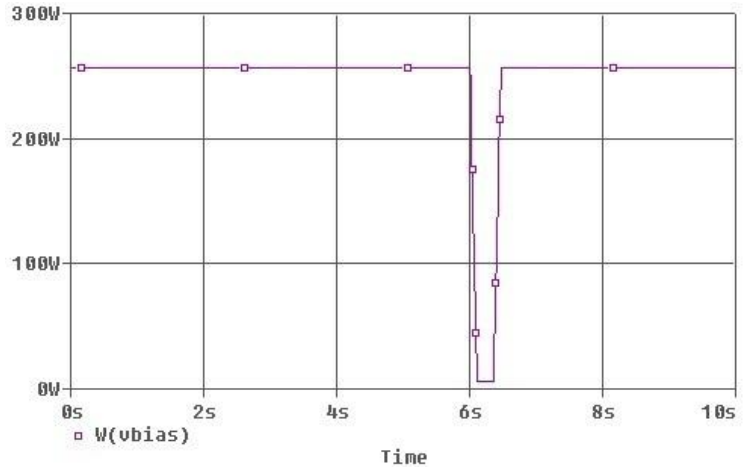

Figure 3-4 Power vs. Time curve (shading effect caused by a car moving over the solar panel with a velocity of 50 km/hr.)

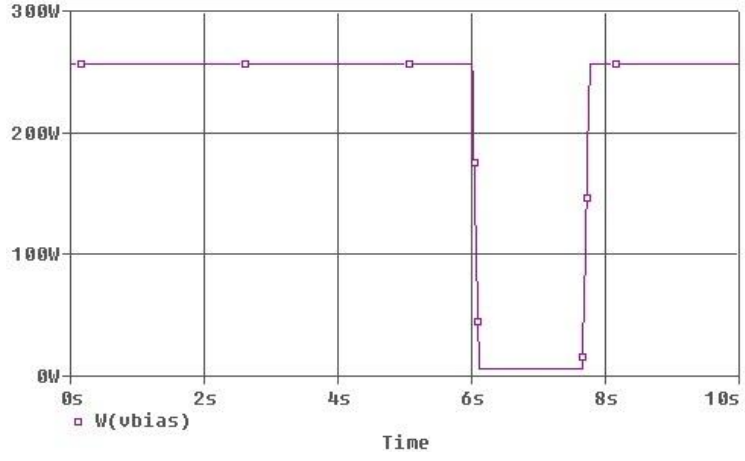

Figure 3-5 Power vs. Time curve (shading effect caused by a tractor semi-trailer moving over the solar panel with a velocity of 50 km/hr.)

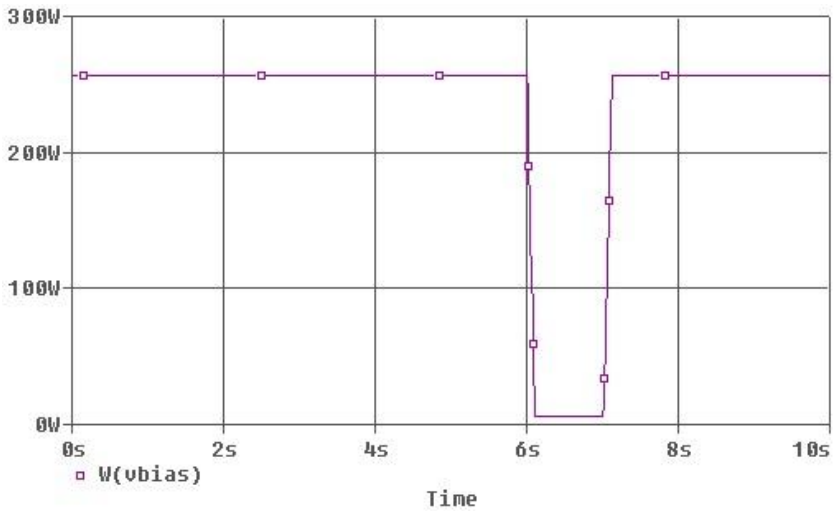

Figure 3-6 Power vs. Time curve (shading effect caused by an intercity bus moving over the solar panel with a velocity of 50 km/hr.)

3.6.3 Experimental study of the effects of fast moving shade

An experimental study to compare the PSpice simulation results obtained for the fast moving shades on the solar panels is carried out. This experiment is conducted inside the laboratory by simulating typical real life conditions of what the solar panels laid on the roads for the Solar Roadways application will face, when a car moves over it. The experiment is conducted inside the laboratory so that all of the conditions that the solar panel could face, such as varying intensity of the light, position of the light, speed with which the car is travelling over the solar panels can be simulated inside the controlled environment.

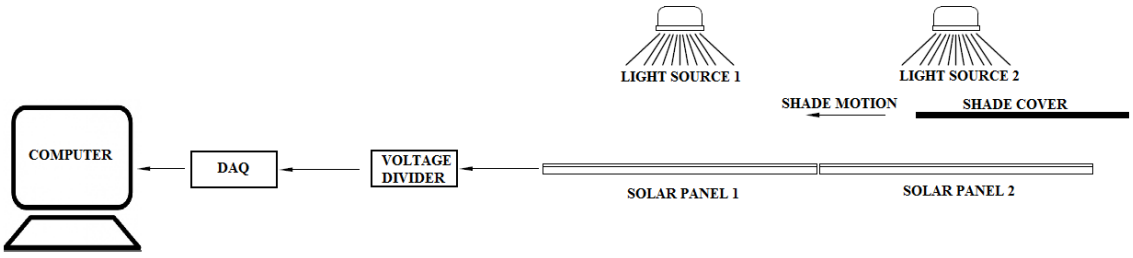

Figure 3-7 Experimental setup for fast moving shade analysis

3.6.3.1 Experimental setup

As shown in Figure 3-7, for the experiment two solar panels of KYOCERA KD135GX-LFBS each with a maximum power output of 135W were selected. In order to simulate the sunlight, two 1000 watts portable halogen lights were used. A multifunction data acquisition system PCI-MIO-16E-4 along with LabVIEW software is used. The DAQ card with 16 analog input channels has a sampling rate of 500kS/s and bipolar input range of ± 5V. The data acquired from the experiment are stored in a computer for future analysis. As the data acquisition system has a limitation of handling ± 5V and each solar panel has an open circuit voltage of 22.1V, suitable voltage divider circuits are employed.

a) Two solar panels connected in series b) Single solar panel

Figure 3-8 Voltage Divider circuit to reduce the voltage for DAQ

Figure 3-8 (a) illustrates the voltage divider with two resistors of value 100 k ohms and 10 k ohms, used for two solar panels connected in series. While Figure 3-8 (b) depicts a voltage divider with two resistors of value 50k ohms and 10k ohms, used for a single solar panel. For simulating a moving car, two sizes of cardboard sheets are used. This is mainly because of the space constraint in using a larger size cardboard sheet, when two solar panels are connected in series. These sheets are moved manually between the halogen light and the solar panels, in order to simulate the car moving over the solar panels and blocking the sunlight falling on it.

3.6.3.2 Experiment

In order to suitably compare the results from the PSpice two types of experiments are conducted. In the first experiment, one KYOCERA KD135GX-LFBS solar panel and two 1000 watts portable halogen lights were used. For representing a car moving over the solar panels a card board sheet of length equal to the length and width of the solar panel is moved at a speed of 0.611 m/s (2.2 km/hr.). Voltage divider circuit as shown in Figure 3-8 is used to reduce the voltage output from the solar panel to below 5V, so that the output from the solar panels can be recorded in the computer using the pc based data acquisition system and the LabVIEW software.

In the second experiment, two KYOCERA KD135GX-LFBS solar panels are connected in series and two 1000 watts portable halogen lights, one for each panel were used. For representing a car moving over the solar panels, a card board sheet of length 0.8m and width of 0.49m is moved over the solar panel at a speed of 0.611 m/s (2.2 km/hr.). Voltage divider circuit in Figure 3-8 is used to reduce the voltage output from the two solar panels connected in series to below 5V, so that the output from the solar panels can be recorded in the computer using the pc based data acquisition system and the LabVIEW software.

3.6.3.3 Comparison of results

Figure 3-9 shows the power vs. time curve obtained in the first experiment. The maximum power output from the solar panel, is 69W. This low power output is mainly due to the low intensity of the artificial lights used to simulate the sunlight. The power output from sunlight can be clearly seen in the Figure 3-3 where the maximum output from the solar panel has been shown to be 135W when simulated in the PSpice with a solar irradiance of 1000 W/m^2. In Figure 3-9 the fall and rise in the power output from the solar panel has taken 5 seconds, primarily due to speed at which shade moved over the solar panel in the experiment. The output from the solar panels reached 15W the lowest value when the solar panel is fully covered. Although a value of zero is expected for the output power when the panel is fully covered, small amount of light that leaks through the sides create a minimal power of 15W. In comparison, Figure 3-4 obtained

via PSpice the output from the solar panels reached closer to 0W when the solar panel was fully covered. Further the energy loss of approximate 55J is present for a solar panel used in the experiment, when it is fully covered with shade. But in the PSpice simulation there is an energy loss closer to 110J is observed, when it is fully covered with shade. This difference in the energy loss may be attributed to the difference in the solar irradiance level used in the PSpice and in the experiment.

Figure 3-10 show the power vs. time curve for the second experiment. The maximum power output from the solar panel, is 120W. This low power output is mainly due the low intensity of the light, from the artificial lights used to simulate the sunlight. This can be clearly seen from Figure 3-4 obtained via PSpice were the maximum output from the solar panel has been shown to be 270W when simulated in the PSpice with a solar irradiance of 1000 W/m^2. The energy loss of approximately 25J is present for the solar panels used in the second experiment due to shade. But in the PSpice simulation there is an energy loss was roughly 250J, when it is covered with shade. This difference in the energy loss is mainly due to the difference in the solar irradiance level used in PSpice and the experiment. In experiment the solar panel was only partially covered with shade, but in PSpice simulation the solar panel was fully covered with shade.

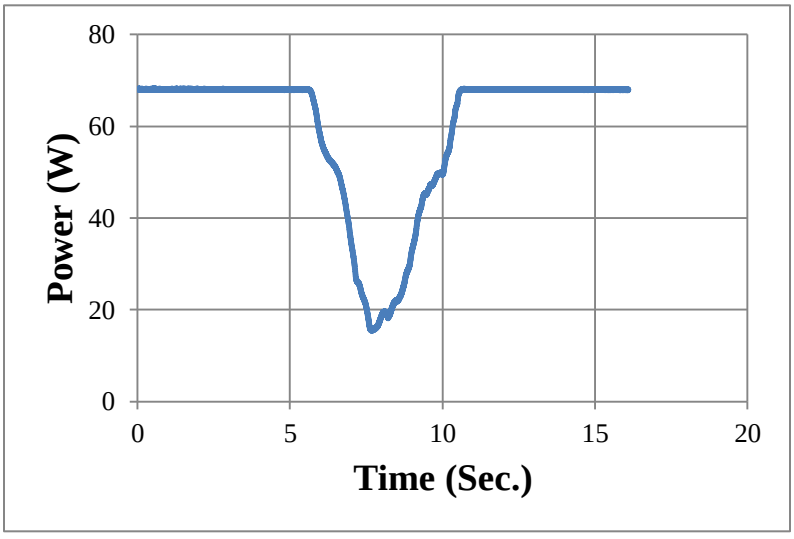

Figure 3-9 Power vs. Time curve for a single solar panel covered by a moving shade

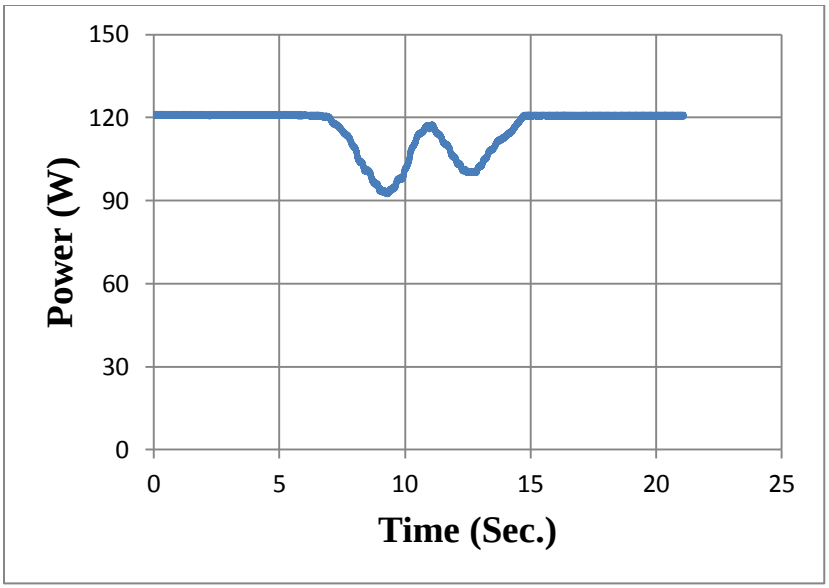

Figure 3-10 Power vs. Time curve for two solar panels covered by a moving shade

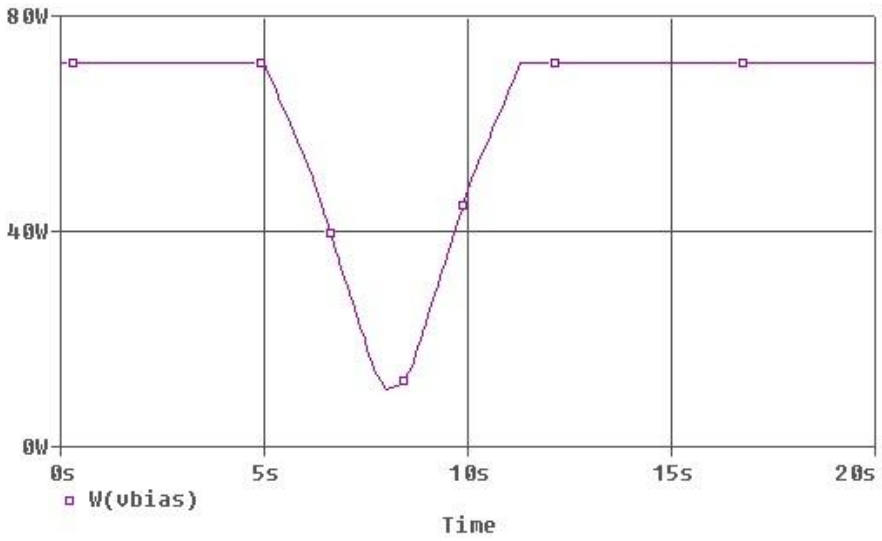

Figure 3-11 Power vs. Time curve from PSpice for a single solar panel covered by a moving shade in PSpice

Figures 3-11 and 3-12 are the results from PSpice, simulated under the conditions similar to the conditions in the experiment. In this simulation the solar irradiance value has been reduced to match the value of the light intensity of artificial lights used in experiment and the speed of the vehicle moving over the solar panels were also reduced in PSpice to match the speed of vehicle used in experiment.

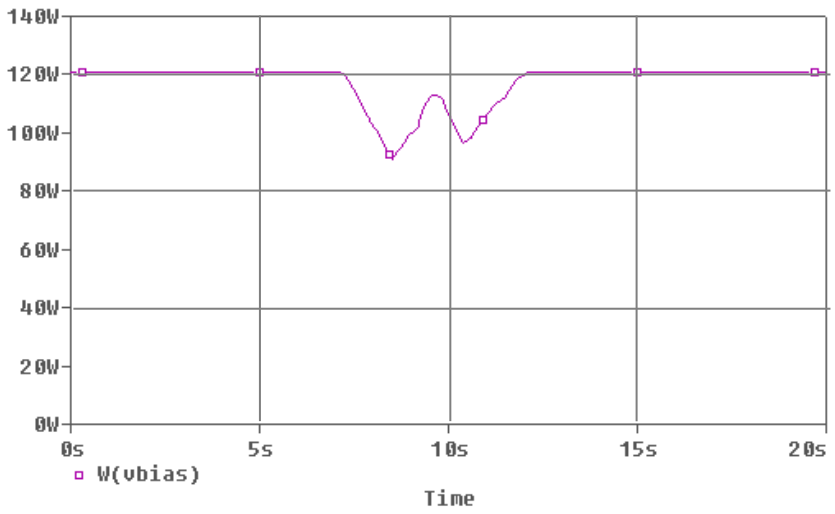

Figure 3-12 Power vs. Time curve from PSpice for two solar panels covered by a moving shade

3.7 **Temperature effects**

The operating temperature of the solar cells at standard test condition is 25° Celsius [4]. Only at this temperature the efficiency of the solar cells to convert the sunlight falling over it into electricity is at its maximum. For every degree Celsius increase in temperature, there will be 0.44% decrease in the maximum power output of the solar cells [30]. Figure 3-13 show the output from the solar panels when the cell temperatures are 25° Celsius and 50° Celsius. It can be clearly seen from the figure that, the output from the solar panels have decreased from 135W to less than 120W with the increase in temperature from 25° Celsius to 50° Celsius. But in Canada, the temperature goes above 25° Celsius only during the months of summer. In all the other months the temperatures are well below the 25° Celsius mark and are sunny, which is most suitable climatic conditions for the solar panels. This will make the Solar Roadways applications even more suitable for Canada.

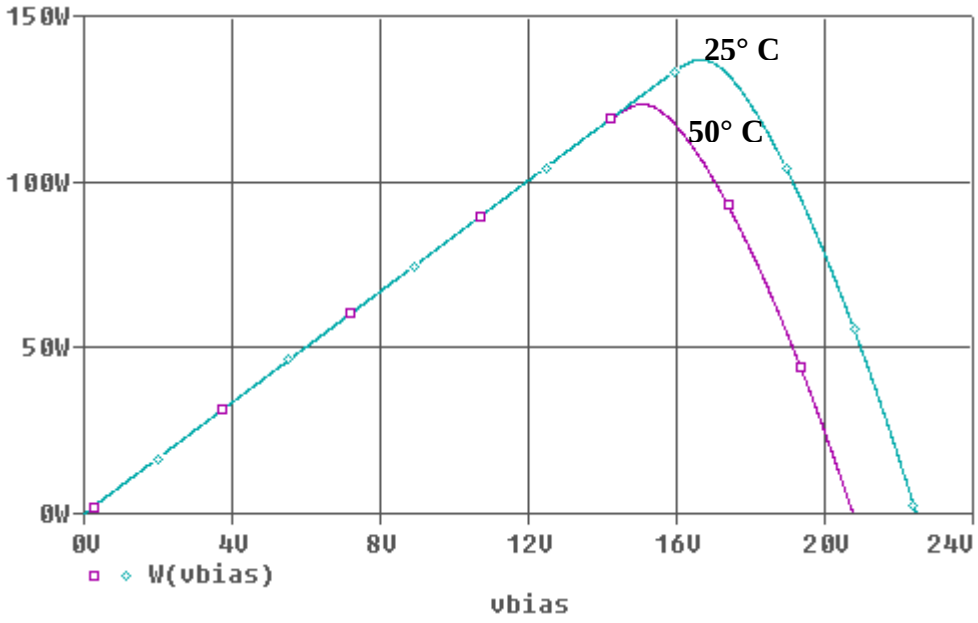

Figure 3-13 Power vs. Voltage curve from PSpice for a selected Kyocera KD135SX-UPU solar panel at 25° C and 50° C

3.8 **Power fluctuation due to panel and other environmental influence**

Apart from the power losses due to the shade, several other losses such as soiling effect, mismatch effect, impact of tilt angle and inverter efficiency can add up to decrease the overall efficiency of the power produced through solar panels. Apart from inverter efficiency all of the other losses are closely associated with solar panels. These losses have to be accounted for prior to implementing a workable efficient Solar Roadways system.

3.8.1 Soiling effects

It is known that 5 - 15% loss of power output is present in the solar panels due to the particulate build up on the solar panel top cover [31]. These particulate build up reduces the amount of sunlight from reaching the solar cells. In Solar Roadways application solar panels are to be laid on the roads which are frequently traveled, and hence there is always a high chance of reduction in the power output due to the soiling effect. Thus, for Solar Roadways application, it is important to perform regular cleaning of glasses to keep itself free from the dirt. It may be noted that for the traditional panels, the glasses come with

thin Titania film coating which can chemically break the down the dirt collected on the surface by using the ultraviolet rays in the sunlight falling over them. [32].

3.8.2 Tilt angle effects

Tilt angles are important data for solar panels, as they can affect the annual output from the solar panels [33].The solar panels produce more power output when they are placed in such an angle that the sunlight falling on the solar panel is always perpendicular to the surface of the solar panels. For a flat mounted system there is an average annual loss of 11% in the power produced by the solar panels [31]. These losses due to tilt angle effects are also called cosine loss. When the panels are at an angle to the sun and not perpendicular to the sun, available energy is reduced and the net energy can be expressed approximately as a function of the cosine of the angle between the sun's rays and the direction of normal to the panel surface. [34]. In solar roadways application, the solar panels are laid over the road, hence they can be considered to be always in a horizontal position. This can result in significant loss in the power that can be extracted from the solar panels.

3.8.3 Mismatch effects

Mismatch losses mainly occur when two modules with different properties or different working conditions are connected together. As Solar Roadways application involves a large number of solar panels connected together, possibilities for mismatch losses to occur are quite high. Mismatch losses are serious effects in large solar arrays, as the output of the entire array is heavily dependent on the output of the solar panel with the lowest output. This will cause the power produced by the normal solar panels to dissipate as heat and may result in permanent damage of the solar panels. In practice, bypass diodes are used to overcome these mismatch effects. Hence the bypass diodes should be rated properly so that they can take on all the current from the array which works properly. Blocking diodes can also be used along with the bypass diodes to prevent the mismatch effects [27].

3.8.4 Inverter efficiency

Inverters are required in grid connected solar system to convert the DC current produced by the solar panels into AC power which is used in the grid system. Inverter efficiency depends on how the inverters convert DC into AC current without any losses. It may be noted that, at present, there are inverters with efficiency up to 98.5% are available [35]. Most inverters are known to be more efficient when they operate close to the full load conditions [36]. Hence it's important to select an inverter which has the power range closer to the power output from the solar arrays.

3.8.5 Transmission losses

It is known that a power loss of 7 to 9 % is present in the electricity generated in the Ontario province alone due to the power being transmitted over a long distance and also due to the heat generated at various points of the grid. These losses even rise to 20 to 25 % during the peak hour periods [37]. But as the Solar Roadways application is to be installed close to the highly populated areas, transmission of electricity over long distance may be avoided and hence the losses minimized.

3.9 Uncertainty Analysis

In order to study the influence uncertainties present in the solar irradiance values, Monte Carlo analysis that is available within the PSpice software environment is employed. Monte Carlo analysis is a type of risk analysis which can predict the outcome of an uncertainty in any problem that cam be modeled mathematically. Monte Carlo analysis give a range of outcomes from an unknown parameter, based on which decisions can be made, on how the system will work in the extreme conditions i.e. at the worst cases which the system might not even experience. In Monte Carlo analysis, the uncertain parameter is usually varied by employing a probability distribution function. In the case of solar panels, solar irradiance value is always an uncertain parameter. Hence, in order to find the power output based on different solar irradiance values Monte Carlo analysis is used. A special command available in PSpice is employed to perform the Monte Carlo analysis [38] which takes the following form:

.MC <#runs value> <analysis> <output variable> <function> [option] [SEED=value]*

The description for the Monte Carlo analysis command used in PSpice is given in Table 3-3. In the equivalent electrical circuit of the solar panel, the Monte Carlo analysis for different solar irradiance value is performed by connecting a resistor along with the voltage controlled current source, so that the current produced by the solar irradiance is varied within a given tolerance value and by a probability distribution function[9]. Based on this variation in the current produced by the PV cells due to the change in the solar irradiance value incident on it, we can study the variation in the power produced by the solar module.

Table 3-3 Description for the Monte Carlo analysis function

Monte Carlo analysis function	**Description**
<#runs value>	The total number of values for which the analysis has to be performed was taken as 5.
<analysis>	Type of analysis to be performed. They are either dc analysis or ac analysis or transient analysis in PSpice. dc analysis was taken for the analysis performed.
<output variable>	Gives what type of output is required in the output file.
<function>	Specifies operation to be performed on the output variable values. YMAX function was used in the analysis. This function computes the absolute maximum difference between the nominal and each run.
[option]	List all the values of random variables used in the beginning of each run.
[SEED=value]	It is an odd integer in between 1 to 32767, which is used in the random number generation within the Monte Carlo analysis. The default value 17533 was taken for the analysis.

The total number of steps performed in this analysis is 5 and the initial condition is maintained to be at the standard test condition of solar irradiance of 1000 W/m^2, air mass 1.5 and cell temperature of 25° Celsius. Gaussian distribution function has been used in order to select the random values and tolerance of 40% is selected for the resistors. Figures 3-14 and 3-15 shows the Power vs. Voltage curve and Current vs. Voltage curve, based on the randomly selected solar irradiance value, by the Monte Carlo analysis for the two selected solar panels of Kyocera KD135SX-UPU connected in series is shown below.

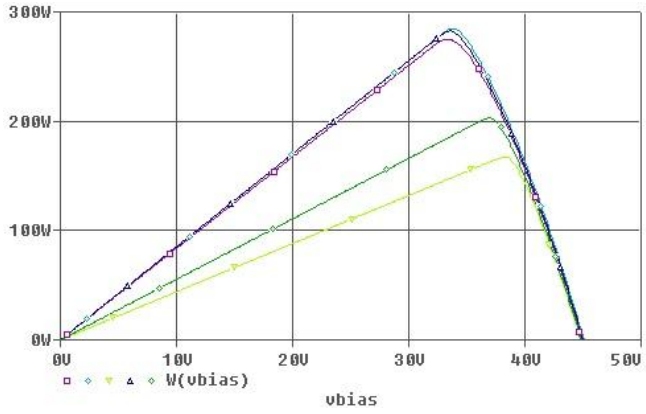

Figure 3-14 Power vs. Voltage curve for a selected Kyocera KD135SX-UPU solar panel with different solar irradiance values(□ -1000 W/m^2, ◇ -1800 W/m^2, ▽ -526.1 W/m^2, △ -1255 W/m^2, ◊ -661.4 W/m^2)

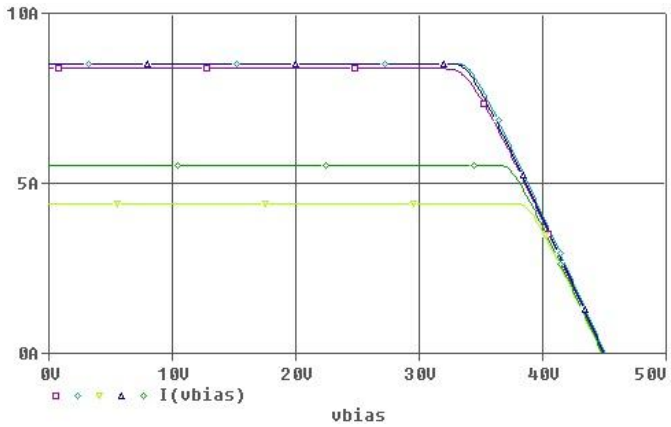

Figure 3-15 Current vs. Voltage curve for a selected Kyocera KD135SX-UPU solar panel with different solar irradiance values

The outputs of two solar panels when connected in series are to be around 270W at the standard test condition solar irradiance value of 1000W/m^2. When the solar irradiance value reaches higher than the standard test condition value, the output from the solar panel didn't raise much and continued to be around 270W. But when the solar irradiance values are lower than the standard test condition value, the output from the solar panel reduced drastically and reached 150W. This variation in the solar panel output is may primarily be attributed to the probability distribution function and the tolerance value for the resistor selected as part of the Monte Carlo analysis.

3.10 **Summary**

In this chapter, effect of fast moving shade on the output of the solar panels, caused by the vehicle moving over it and various other losses that are involved in the Solar Roadways application has been studied. The amount of energy loss in the solar panels has been found to be dependent on the lengths and speeds of the vehicle. Other losses such as temperature effect, mismatch effect, impact of tilt angle and inverter efficiency can add up to decrease the efficiency of the solar panel to produce electricity. Monte Carlo analysis which is a risk analysis method was used to predict the outcome by the varying values of the solar irradiance falling over the solar panel. This analysis showed how the solar panels behave when the solar irradiance value are higher or lower than the standard test condition value of 1000 W/m^2.

Chapter 4

4 Static and Dynamic Characterization via COMSOL

4.1 Introduction

Solar panels for the current power generation applications are built to take on loads due to hail, the weight of collected snow and strong winds. However, in the solar roadways application additional loads such as the load due to vehicle moving over it and people walking over it are present. In other words panels have to withstand loads that are normally taken by the roads and walkways in addition to the typical environmental loads. Thus, the solar panels to be used for this application, must have the necessary structural strength to take on the vehicle load moving over it while possessing surface properties similar to those of traditional roads, so that the vehicles moving over it will have sufficient traction to move and stop safely in slippery conditions like rain and snow. To satisfy these requirements, it is quite obvious that the traditional materials that are used for manufacturing the current solar panels are not suitable for solar roadways applications. Hence, there is a need for studying the load carrying capacity of the existing glasses and other transparent materials that are available at present that can be used as a cover for the solar panels. COMSOL Multiphysics which has both the modeling and simulation capabilities for Multiphysics systems is used in the present study to ascertain the feasibility for different vehicular applications and for suggesting future material and geometrical properties.

4.2 COMSOL Multiphysics

COMSOL Multiphysics is engineering simulation software, which has the capability to analyze engineering problems that require many physics to be coupled together. This software has easy steps for modeling the geometry, defining their material properties, meshing, specifying their physics, solving and visualizing results [39]. In the present analysis, structural mechanics module of COMSOL Multiphysics has been employed. In particular, this module is used to study deflection under typical loads encountered in solar roadways application. The structural mechanics module has many study types, such as stationary, Eigen mode, parametric, quasi-static, transient, frequency response and pre-

stressed included in it. This module also has an interface for the piezoelectric devices which is employed for investigating the possible mechanical stress induced energy harvesting from the solar panels.

4.3 **Panel model for COMSOL analysis**

The basic solar panel consists of solar cells which are permanently encapsulated between a tempered glass cover plate and a back sheet which is secured in an aluminum frame [28]. Similarly, the solar roadways panel must also have strong base layers which can hold the solar cells and their related electrical systems to tap the power produced by the solar cells and connect it to the grid connector system. In order to cover this base layer, a top cover plate must be utilized. This plate must be transparent enough to allow the sunlight to pass through it and also have high strength to withstand the load of vehicles passing over it. In addition, this top cover plate must also be sufficiently rough in order to provide enough traction for the vehicles [1].

The model created in the COMSOL Multiphysics shown in Figure 4-1 for the analysis purpose consists of a vertically hollow square base layer with sides 4 meters in length, 0.5 meter in height and 0.1 meter in thickness. This base layer is considered to be made up of concrete, and covered with a transparent cover of size 4 meters and thickness 0.01 meter made up of acrylic plastic, whose material properties are given in Table 4-1. The acrylic sheets have a working temperature range of -40°C up to 93°C [40], and the elastic properties are assumed to remain constant in this temperature range.

Table 4-1 Material properties for Acrylic plastic and Concrete

Material Properties	**Acrylic plastic**	**Concrete**
Density	1190 (kg/m^3)	2300 (kg/m^3)
Young's modulus	$50.8x10^9$ (Pa)	$25x10^9$ (Pa)
Poisson's ratio	0.37	0.33

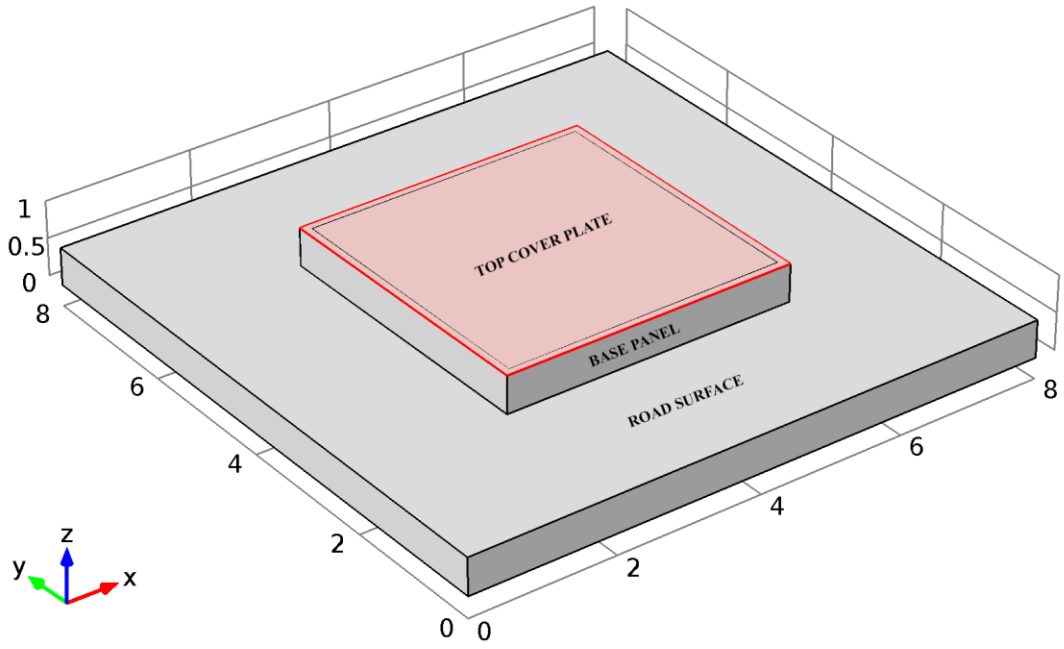

Figure 4-1 Solar Roadways panel model for COMOSL Multiphysics analysis

4.4 Selection of Standard Loads for solar roadways panel analysis

As the solar roadways panels are to be laid over the existing roads, the primary loads acting on the solar roadways panels are the vehicle loads. For the analysis, the loads associated with the vehicles are selected based on the specification from American Association of State Highways and Transportation Officials (AASHTO). Two types of loadings, H loading and HS loading are given by AASHTO [41]. H loading consists of a two axle truck and HS loading consists of a tractor truck with semi-trailer. In general, there are four standard classes of highway loading conditions, namely H15, H20, HS15 and HS20. The number following the H and HS letter denotes the gross weight in tons of a standard truck. In the analysis of the solar roadways panel using COMSOL Multiphysics, H20 loading standard as displayed in Figure 4-2 is used. The gross weight of the truck is taken to be 18143.7 kg (40000 lbs.), while the front and the rear axle weights are respectively 3628.7 kg (8000 lbs.) and 14515 kg (32000 lbs.).

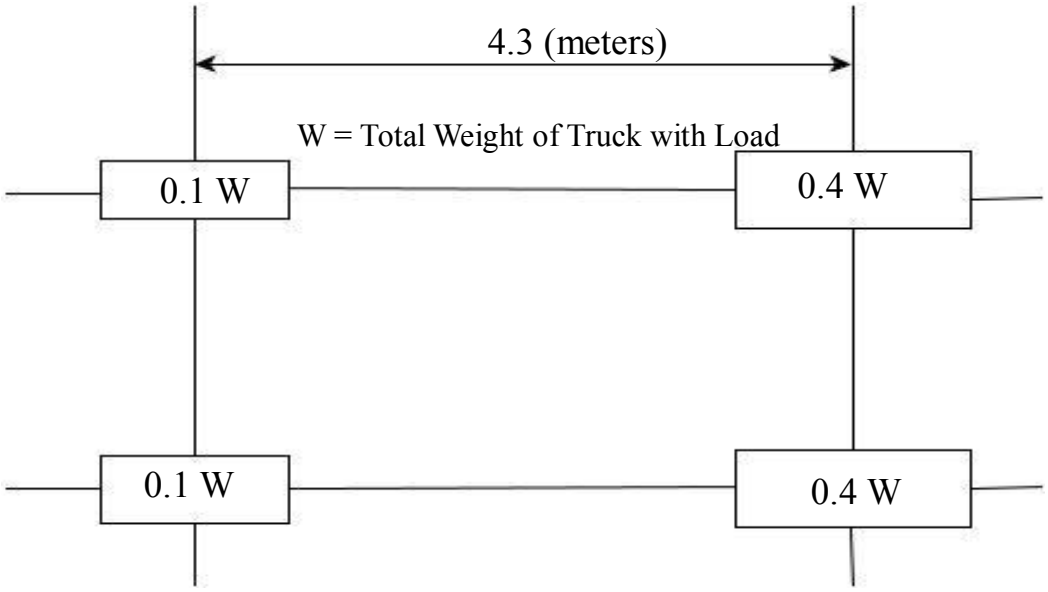

Figure 4-2 Standard H truck loading taken from Standard Specifications for Highway Bridges by AASHTO [37]

4.5 **COMSOL analysis procedure**

The essential steps involved in the COMSOL Multiphysics analysis are shown in Figure 4-3. The first step in the COMSOL Multiphysics analysis considers the global definitions such as parameters and variables that are used in the analysis. The global parameters such as the weight of the truck and the initial position of the truck front axle, i.e. the position from which the load of the truck start to acts on the solar roadways panel are selected.

The second step defines a model for the solar roadways panel. As part of this step, local definition such as local coordinate system must be also redefined. Then, the geometry of the model is defined using the geometry node in the software. The model consists of a base layer and a top cover plate. The size of the base layer is (4m x 4m x 0.5m) and that of the top cover plate is (4m x 4m x 0.01m). Following the geometry definition of the model, the materials for the base layer and the top cover plate are defined. The base layer

is assigned as concrete material and the top cover plate is assigned as acrylic plastic. Properties of these materials are given in Table 4-1.

Third step in the analysis defines solid mechanics interface properties which resides under the structural mechanics module. These properties include fixed constraints and definition of the positions where load due to vehicle act on the solar roadways panel model. The base layer and all four sides of the top cover are considered to have fixed constraint i.e. the displacements are zero in all directions. Fourth step in the analysis defines mesh elements for the model. Free tetrahedral type of mesh elements is selected and the size of the elements for each boundary was defined separately.

The fifth step in the analysis defines the type of study that has to be performed on the model. In this analysis parametric type of study is performed. The parameter selected for the study is the position of front axle of a truck. For the analysis geometric nonlinearity is also considered, due to possible large displacement to be caused by the truck load. In the final step visualization of the various results and the corresponding analysis is performed.

4.6 **Available glass to cover the solar panel**

The primary purpose of the top cover plate used in the solar panels is to protect the solar cells from getting damaged by the external loads such as collection of dust or snow and the load due to heavy wind. The solar panel top cover must also be transparent enough to allow maximum amount of sunlight to pass through it, so that the efficiency of the solar cells is not reduced. In order to take up sufficiently large loads, while being transparent, tempered glasses are mostly used as solar panel top cover [28]. Tempered glasses are also called as toughened glasses which are physically and thermally stronger than the normal glasses. In typical solar panels that are currently in production, acrylic glass sheets are also used which are lighter than tempered glass and has physical properties similar to it. In the present study, acrylic glass material is selected for the analysis. The properties of the acrylic glass material given in Table 4-1 are employed.

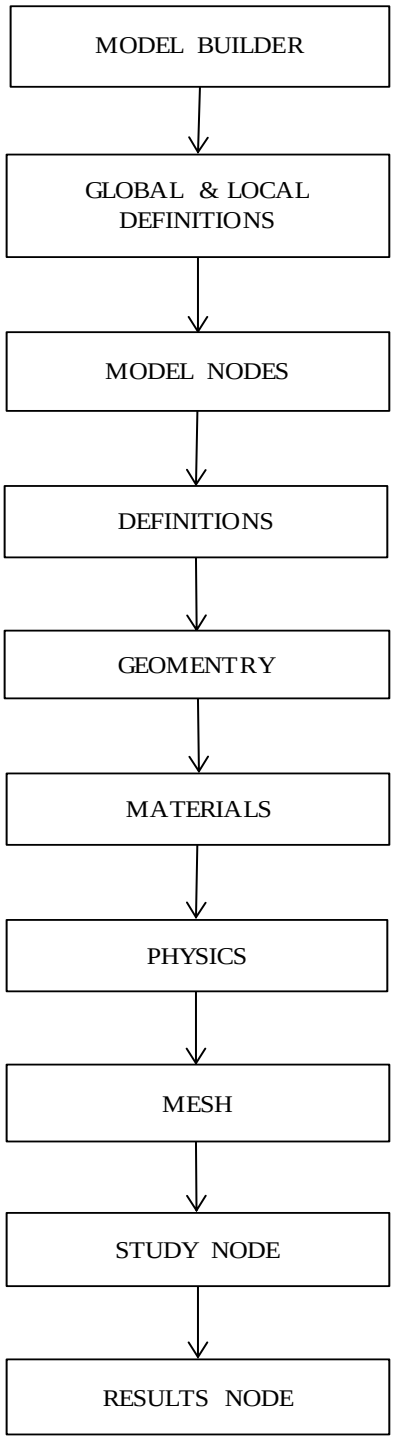

Figure 4-3 Steps involved in COMSOL Multiphysics analysis

4.7 **Analysis of load carrying capability**

The load carrying capability of the selected acrylic glass sheet, for the solar panels in the solar roadways application, is investigated using the COMSOL Multiphysics software. Based on the model of the solar panel for the solar roadways and the standard HS20 loading conditions, the load carrying capability of the acrylic glass sheets are studied. As the standard length of the truck used in HS20 loading condition is 4.3 m, which is longer than the length of the solar panel modeled for the solar roadways, only one axle weight acts on the solar panels at any given time. Hence the rear axle, where a larger proportion of the weight of the truck acts is taken for the analysis. According to Beer-Lambert law given in equation 4-1, the absorption of the light passing through a material depends on the property of the material and the path length of the light [42]. In order to allow maximum light to pass through the acrylic top cover of the solar panel such that the solar cells receive maximum sunlight and generate more electricity, the thickness of the top cover is selected as 10mm. The relation between the thickness of the material and its light transmission ability is given by

$$\mathbf{I} = \mathbf{I_0} e^{-\alpha x} \quad , \tag{4-1}$$

where **I** is the measured intensity of the light transmitted through a layer of material, $\mathbf{I_0}$ the intensity of the light incident on the material, α the absorption coefficient and x the thickness of the material.

When the HS20 standard truck load is applied on the acrylic sheet in COMSOL, the effect of the truck load on the acrylic sheet is analyzed for every 0.1 meter and the load is considered to move in the positive x direction. The maximum von Mises stress and the maximum displacement based on the location of vehicle rear wheels is given in Table A-1. Only the load locations that results in maximum von Mises stress and displacement as shown in Table 4-4 are given in the discussion below. The load caused a maximum von Mises stress of 1.82×10^3Mpa as shown in Figure 4-4, is much higher when compared to the ultimate tensile strength of 69Mpa [40] and the displacement results indicate that maximum surface displacement was also very high at 1.12 meters. According to the

AASHTO standards, the allowable deflection for a bridge is span length/800 for vehicular bridges and span length/1000 for pedestrian bridges [41]. It may be noticed that in the present case of the top cover of panel, the maximum displacement is predicted to be approximately span length/3.6 which is much higher than the above standard requirements. Hence it can be concluded that the selected top cover material is not suitable for the applied load and this cannot be used as a top cover for solar roadways panel, where vehicles of size similar to a truck are moving over it.

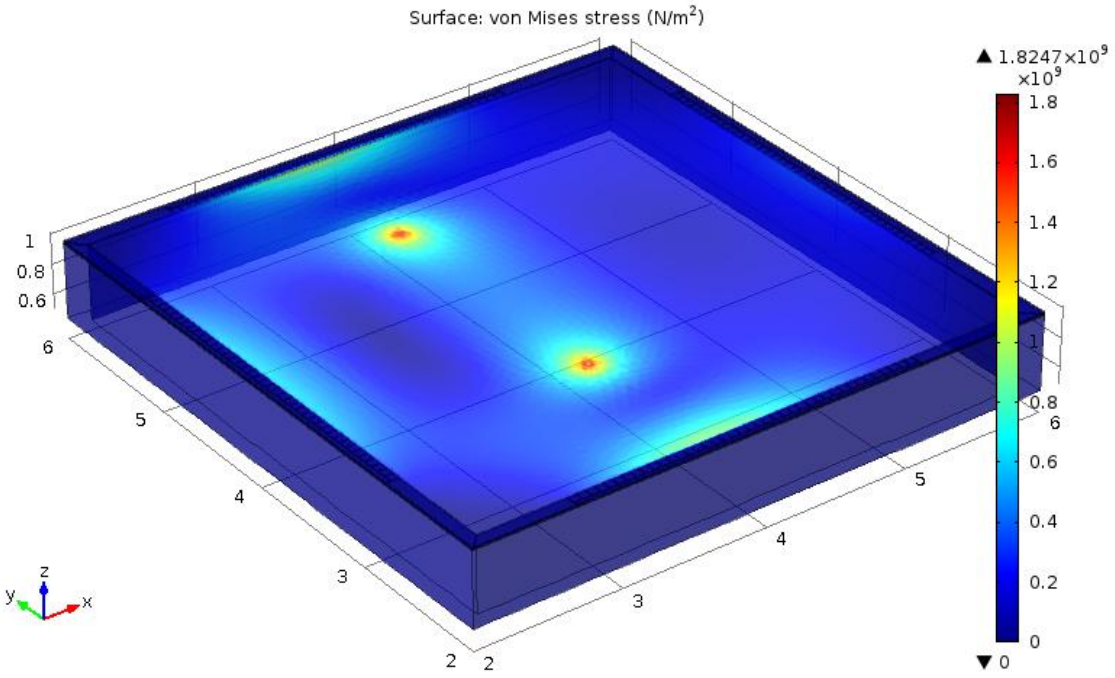

Figure 4-4 Maximum von Mises stress for HS loading of truck on solar panel of the Solar Roadways system (at wheel location of 3.6m)

As the selected material failed for the load of a truck, in order to test the maximum load the material selected for the top cover of solar roadways panel can take on, stress and displacements due to a car load and a motorbike load moving over the solar panel are also analyzed. The load of the Mini Copper car and the load of the Yamaha RZ8 motorbike are selected for the analysis. The specifications for the selected car and the motorbike are given in Table 4-2.

Table 4-2 Specifications of car and motorbike used in the analysis

	Car [43]	Motorbike [44]
Curb weight	616.9 kg (1360 lbs.)	213.2 kg (470 lbs.)
Length	3.05 m	2.1 m
Wheel base	2.04 m	1.5 m
Weight distribution	60/40	51/49

As the wheelbase of the car and the motorbike selected for the analysis are smaller than the length of the solar panel modeled for the solar roadways application, the load due to all four wheels in the case of a car and all two wheels in the case of a motorbike are considered for the analysis. The wheelbase of the car selected for analysis is 2.04 meters as shown in Table 4-2. In this analysis the distance between the front axle and rear axle is maintained at 2.04 meters, so that only after the front wheels enter and travels a distance of 2.04 meters over the solar panel, the rear wheels enter and move over the solar panel. The weight distribution between the front and the rear axles confirm to a ratio of 60 to 40 as shown in Table 4-2. Hence only 60 percent of the total weight of the car is considered to act on the front wheels and the remaining 40 percent on the rear wheels. The motorbike selected for the analysis has a wheelbase of 1.5 meters. In the analysis, the distance between the front and the rear wheels is maintained at 1.5 meters, so that only after the front wheel enters and travels a distance of 1.5 meters over the solar panels, the rear wheel enters and moves over the solar panels. The weight distribution between the front and the rear wheel are in the ratio 51 to 49, and hence 51 percent of the total weight of the motorbike acts on the front wheel and the remaining 49 percent on the rear wheel.

Based on the selected parameters, the load carrying capacity of the material selected for the solar roadways solar panel is analyzed for the load of a car and motorbike moving over it. The front wheels of the car enter at the x position of 2.1 meters and continue to move in the positive x direction. After the front wheels have moved through the wheelbase distance of 2.04 meters over the solar panel, the rear wheel is considered to

enter the solar panel. The maximum von Mises stress and the maximum displacement based on the location of car front wheels is given in Table A-1. As in the previous case, only the load location that results in the largest stress is presented in the thesis as shown in Table 4-4 is given in the discussion below. The load caused a maximum von Mises stress of 117.48Mpa as shown in Figure 4-5, which is quite high when compared to the ultimate tensile strength of 69Mpa [40] and the maximum surface displacement was also found to be very high at 98.19 mm as shown in Figure 4-6. Hence the selected top cover material cannot be used as top cover for solar roadways panel, when vehicles of size similar to a Mini Copper car move over the surface.

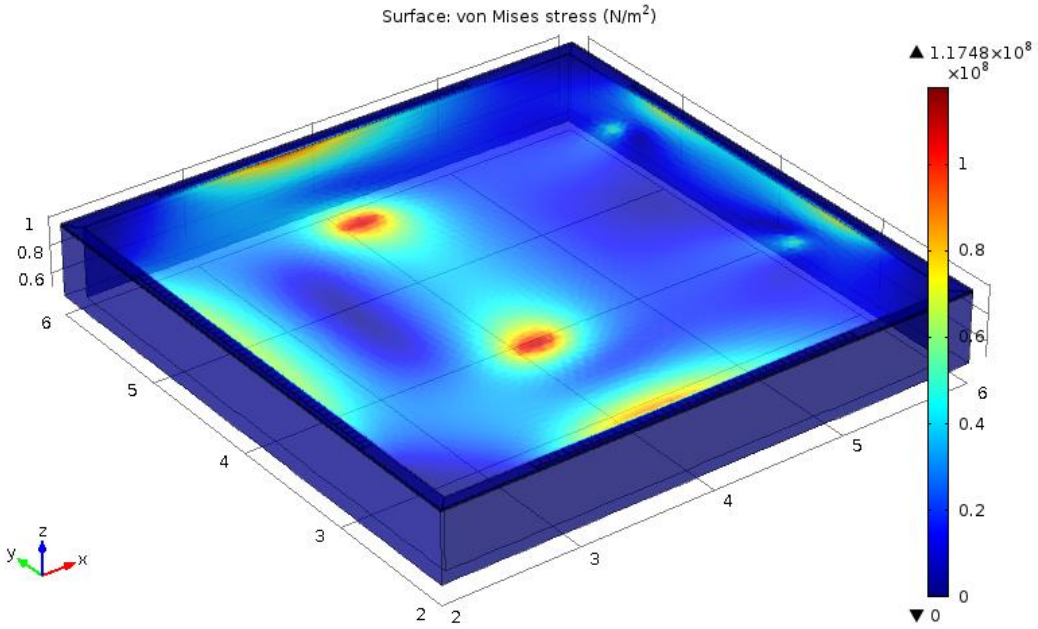

Figure 4-5 Maximum von Mises stress for load of a car on solar panel of the Solar Roadways system (at front wheel location of 5.5m)

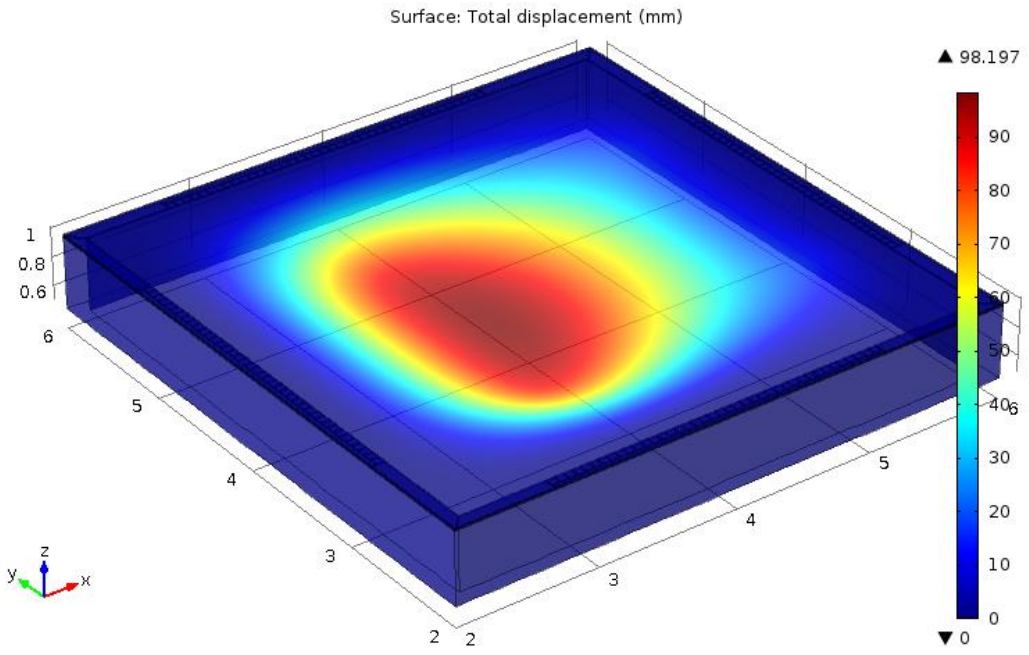

Figure 4-6 Maximum displacement for load of a car on solar panel of the Solar Roadways system (at front wheel location of 5.5m)

Based on the selected parameters, the load carrying capacity of the material selected for the solar roadways solar panel has been analyzed when a load that represents a motorbike move over the panel. The front wheel of the bike enters at the x position of 2.1 meters and continues to move in positive x direction. After the front wheel has moves a distance of 1.5 meters over the solar panel, the rear wheel is considered to enter the solar panel. The maximum von Mises stress and the maximum displacement based on the location of the motorbike's front wheel is given in Table A-1. As in the previous case, only the load location that results in the largest stress is presented in the thesis as shown in Table 4-4 is given in the discussion below. It may be noted that the load resulted in a maximum von Mises stress of 65.5Mpa as shown in Figure 4-7, this value is quite close when compared to the ultimate tensile strength of 69Mpa [40] and the maximum surface displacement has been found to be quite as high at 39.5 mm as shown in Figure 4-8. It is known that it is best to avoid the large deflections in the top cover in order that the vehicle tire rolling up on a slope and as a result increasing the fuel consumption of the vehicle may be

minimized [45]. Based on the predictions, it may be concluded that the selected material cannot be used as top cover for the solar roadways panel, where the vehicles of size similar to a Yamaha RZ8 motorbike move over the panel.

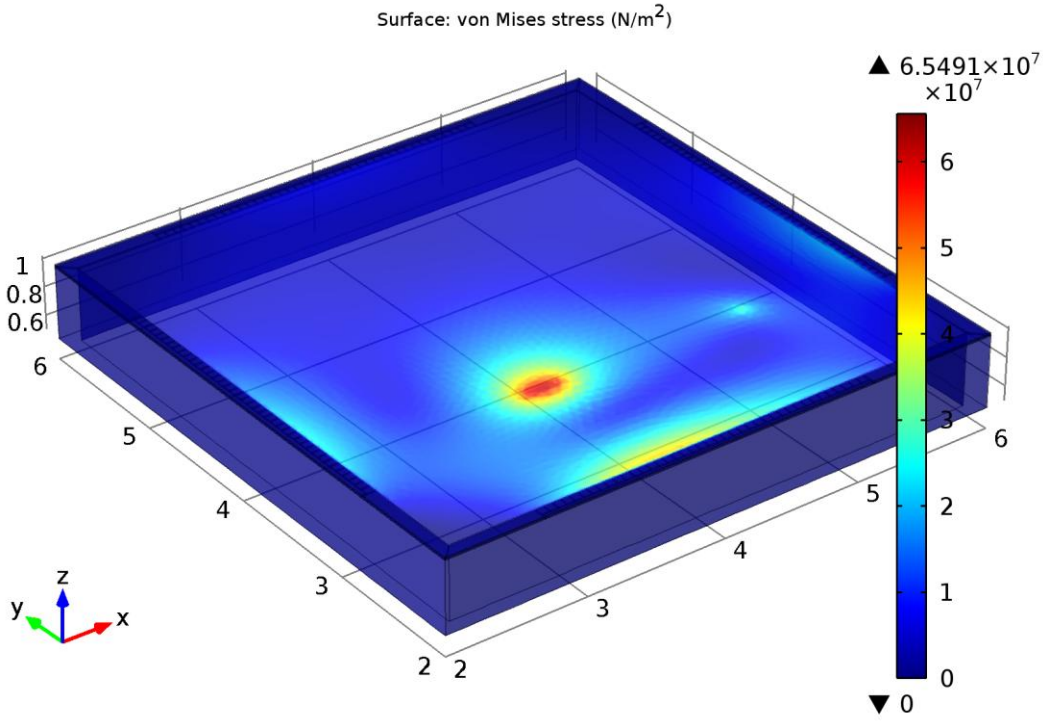

Figure 4-7 Maximum von Mises stress for load of a motorbike on solar panel of the Solar Roadways system (at front wheel location of 5m)

It may be noted that the reduction in the load induced stress levels and the maximum deflection levels in the selected top cover material may be achieved by increasing the thickness of the top cover, while compromising the amount sunlight that can pass through it and reach the solar cells. For the increased thickness analysis, 15 mm and 25.4 mm thick plates are selected. Two individual cases of load of a car and of a motorbike moving over the solar panel are analyzed employing methods discussed earlier.

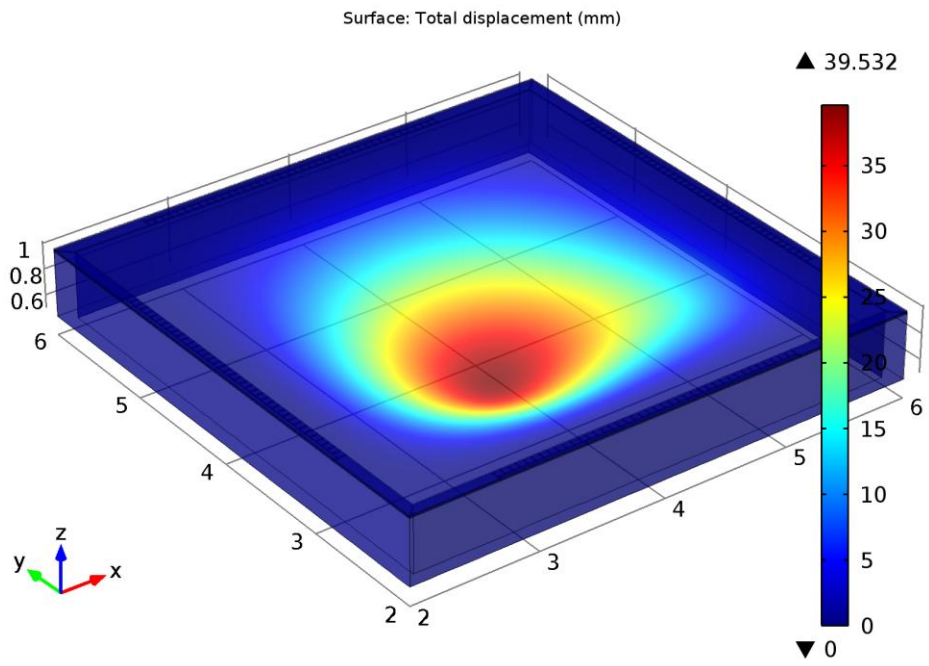

Figure 4-8 Maximum displacement for load of a motorbike on solar panel of the Solar Roadways system (at front wheel location of 5m)

The increase in the thickness of the material selected for the solar panel top cover shows a drop in the maximum von Mises stress and deflection of the top cover. When the load of the car is applied on the top cover with thickness of 15 mm, the maximum von Mises stress reduced to 52.8Mpa as shown in Figure A-1, which was still quite close to the ultimate tensile strength of the material. The maximum deflection of the material has been found to be 29.2 mm as shown in Figure A-2, which is still high based on the AASHTO standards. When the load of the car is applied on the top cover with thickness of 25.4 mm, the maximum von Mises stress reduced to 18.3Mpa as shown in Figure A-3, and the maximum deflection of the material has been found to be 6.06 mm as shown in Figure A-4, which is close to the deflection based on the AASHTO standards.

When the load of the motorbike is applied on the top cover with thickness of 15 mm, the maximum von Mises stress reduced to 29.4Mpa as shown in Figure A-5, and the deflection of the material was 11.8 mm as shown in Figure A-6, which is still high based on the AASHTO standards. When similar analysis is performed on the top cover with thickness of 25.4 mm, the maximum von Mises stress reduced to 10.2Mpa as shown in

Figure A-7, and the deflection of the material has been 2.4 mm as shown in Figure A-8, which is close to the deflection based on the AASHTO standards. Increase in thickness of the material from 6 mm to 25.4 mm results in reduction of the maximum von Mises stress values below the ultimate tensile strength, while the maximum deflection remains closer to the AASHTO standard value. However, caution must be taken when increasing the thickness since it will reduce the amount of sunlight passing through it as shown in Figure 4-9, and results in a reduction of power output from the solar panels.

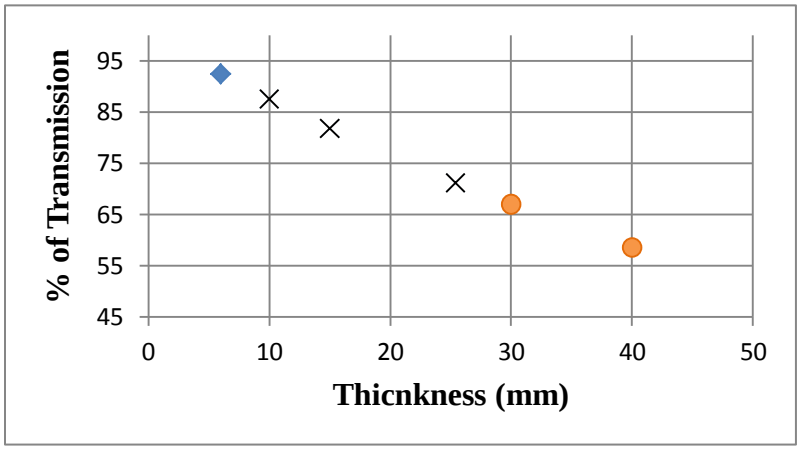

Figure 4-9 Reduction of sunlight transmitted through acrylic sheets with the increase in thickness

(- 6mm thick sheet with maximum transmission of light; - 10mm, 15mm and 25.4mm thick plate used in analysis; - 30mm and 40mm other sizes)

Based on the literature it is recommended that the optimum thickness for the solar panel top cover is to be selected in the range of 2.5 mm to 12 mm [46]. Hence, to achieve reduction in thickness without compromising on the deflection of new material with superior properties must be developed. In the COMSOL Multiphysics the basic properties which are used for the analysis are density, Young's modulus and Poisson's ratio. In order to achieve a reduction in the deflection, the Young's modulus of the material is increased. When the Young's modulus is increased from 50.8×10^9 to 50.8×10^{10} Pa for a solar panel top cover of 15mm thick and load of a motorbike was applied over it, the deflection of the top cover reduced from 11.757 mm shown in Figure

A-6 to 1.176 mm shown in Figure A-9 which is well below the AASHTO standard. If such a material with the increased Young's modulus with the thickness 25.4 mm is used, the load of a car moving over it can be adequately taken up.

In the above analysis, for analyzing the load carrying capability of the commercially available materials only stationary loads of the vehicle have been used and the material failed to take these loads with regards to stress as well as deflection. However, in the future when materials are developed to take on the load of the vehicle over it, then dynamic load (i.e. vehicle moving in space as well as time) must also have to be considered in the prediction of the maximum load carrying capability of the developed material. However, the present stationary analysis can be used in feasibility studies.

4.8 **Solar panel for bicycle lane**

The previous analysis for the top cover material of the solar panels in the solar roadways application demonstrated that, the material for the top cover requires a large improvement in the mechanical properties so that they can take on the vehicle load moving over it while exhibiting surface properties similar to those of present roads, so that the vehicles moving over it will have sufficient traction to move and stop safely during the slippery conditions like rain and snow fall. But the analysis also showed that the commercially available materials have sufficient strength to be laid on the bicycle lanes and walkways. Cities in Canada are developing dedicated bicycle lanes, in order to encourage increased usage of bicycles and for promoting both human and environment health. Hence, laying solar panels over these bicycle lanes can be considered as a viable alternative for producing electricity and also serve their present intended purpose.

A COMSOL study is hence performed to investigate the feasibility. The standard width of the bicycle lanes in Canada are 1.5 meters [47]. To cover these bicycle lanes with the solar panels, a square solar panel of size 1.5 meters is selected. Similar to the solar roadways solar panels, these solar panels are selected to have a vertically hollow square base layer of size 1.5 m x 0.2 m x 0.1 m, which can hold the solar cells and all the electronics which are required for connecting the power produced by the solar cells with the grid. The base layer is covered by a transparent top cover of size 1.5 meters and with

a thickness of 10 mm. The base layer is considered to be made of concrete and the properties used are shown in Table 4-1. For the top cover material, acrylic plastic is considered and the properties are shown in Table 4-1.

Table 4-3 Specifications of bicycle used for analysis

Curb weight	13.6 kg (30 lbs.)
Wheel base	1.006 m
Weight distribution	40/60

For the COMSOL analysis a bicycle with specifications as shown in Table 4-3 was selected. The wheelbase of 1.006 meters is selected for the analysis. In the analysis, the distance between the front and the rear wheels is maintained at 1 meter, so that only after the front wheel enters and travels a distance of 1 meter over the solar panel, the rear wheel enters and moves over the solar panel. The total weight of 90.7 kg (200 lbs.) which includes both the weight of the bicycle and the person travelling on it has been taken for the analysis. The weight distribution between the front and the rear wheels are assumed to be in the ratio of 40 to 60 as shown in Table 4-3. Hence, 40 percent of the total weight of the bicycle acts on the front wheel and the remaining 60 percent in the rear wheel.

The maximum von Mises stress and the maximum displacement based on the location of bicycle front wheel is given in Table A-2. As in the previous case, only the load location that results in the largest stress is presented in the thesis as shown in Table 4-4 is given in the discussion below. The load has been found to cause a maximum von Mises stress of 20.67Mpa as shown in Figure 4-10, which is quite low when compared to the ultimate tensile strength of 69Mpa [40] and the maximum surface displacement was also quite close at 2.05 mm as shown in Figure 4-11, when compared to the AASHTO standard.

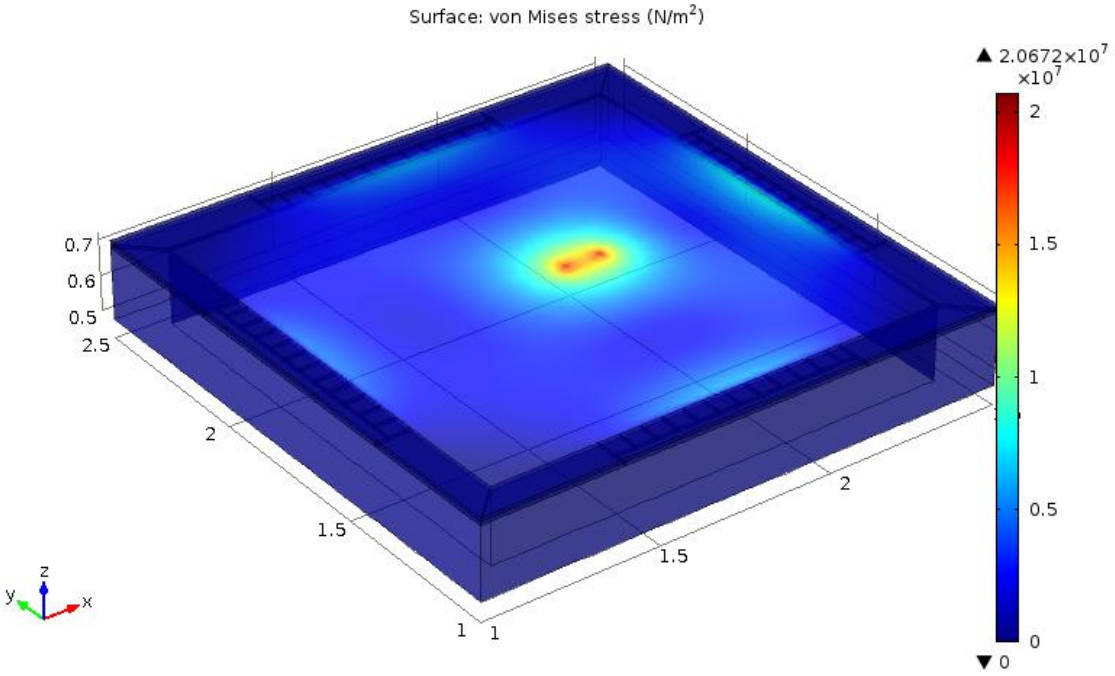

Figure 4-10 Maximum von Mises stress for load of a bicycle on solar panel of the Solar Roadways system (at front wheel location of 2.8m)

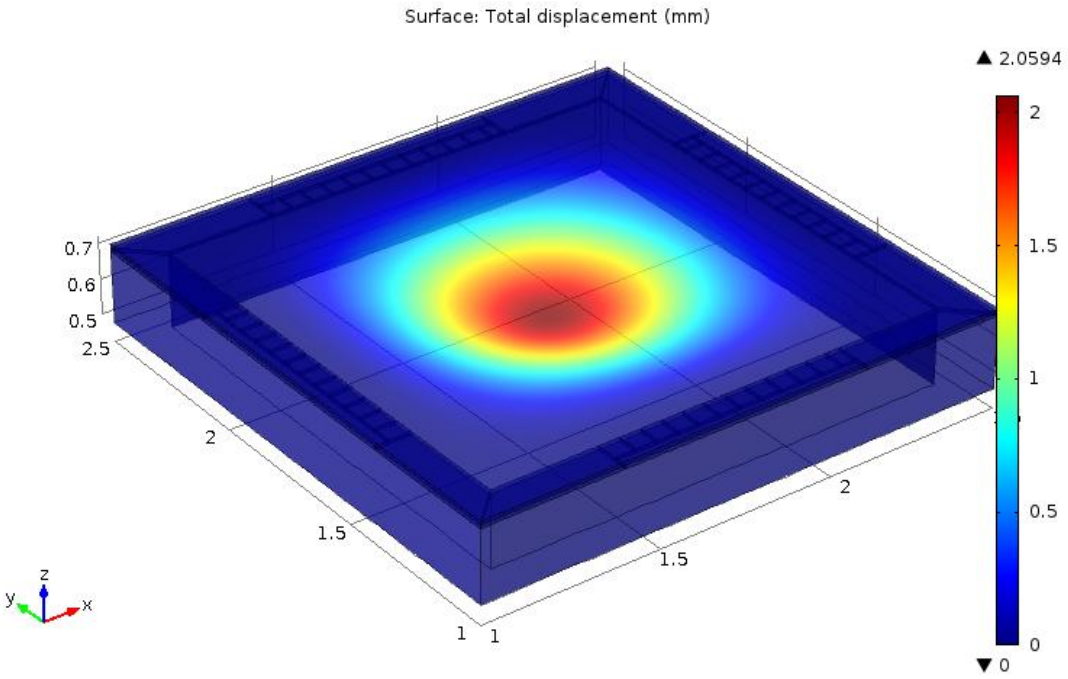

Figure 4-11 Maximum displacement for load of a bicycle on solar panel of the Solar Roadways system (at front wheel location of 2.7m)

Table 4-4 Summary of maximum von Mises stress and displacement for various load cases analyzed in COMSOL

Vehicle type	X position of the front axle (m)	Maximum von Mises stress (N/m^2)	Maximum Displacement (m)
Truck	3.6	$1.82x10^9$	N/A
	4	N/A	1.1222
Car	5.5	$11.7x10^7$	0.0982
Motorbike	5	$6.549x10^7$	0.0395
Bicycle	2.8	$2.06x10^7$	N/A
	2.7	N/A	0.002

4.9 **Summary**

In this chapter, the load carrying capacity of the top cover of the solar panels for the solar roadways application is analyzed using COMSOL Multiphysics software. The primary motivation for the analysis comes from both material characteristics and solar roadways vehicular applications. The acrylic plastic material of 10 mm thickness has been selected for solar panel top cover. It has been demonstrated that this material failed to take the load of a typical truck, car and motorbike moving over the solar roadway top cover. Increase in the thickness of the material resulted in adequate reduction in both the deflection and stress in the material. Increasing the Young's modulus also resulted in a reduction deflection and was suitable for taking the load of the motorbike and car moving over it. As a currently viable option, solar pathway for a typical bicycle lane was modeled considering the same acrylic plastic as solar panel top cover. This panel was able to take up the load of a typical bicycle - person moving over the panel cover.

In chapter 5, an auxiliary energy harvesting model using piezoelectric materials is proposed. This system analyzed using COMSOL Mulitphysics, utilizes the stresses developed during the vehicle moving over the solar panel and produce power. The positions where maximum stresses occur are studied experimentally in an effort to predict optimal placement for these transducers.

Chapter 5

5 Investigation of an Auxiliary Energy Harvesting System

5.1 Introduction

In the solar panels used for the solar roadways application, in addition to the inherent low energy efficiency of the solar panels, losses in the power output due to the shadow, soiling, tilt angle, mismatch effects and etc. have been found to affect the overall efficiency. In order to overcome these losses in the power output, an auxiliary energy harvesting system employing piezoelectric transducers is proposed. This method relies on converting the strain developed in the solar panel top cover into electricity. In order to increase the efficiency of the auxiliary system, the locations of the piezoelectric elements are optimized using COMSOL Multiphysics by selecting the locations along the outer edges of the panel. In particular among these available edge locations, positions where high stresses act due to the load of the vehicle over the top cover of the solar panel are of interest. Optimized positions of the piezoelectric elements are also obtained experimentally using a modal analysis approach employing frequency response as well as a transient approach where the excitation is provided by experimentally simulating the moving loads. In both cases, a scanning Laser Doppler Vibrometer (LDV) system has been used for non-contact measurement of panel vibration.

5.2 Piezoelectricity

Piezoelectricity is a property exhibited by certain materials such as crystals or ceramics which produce charge when mechanical strain is applied. In piezoelectricity, in general two types of effects are considered. The first type is the direct piezoelectric effect, where mechanical stresses due to the external load applied on the piezoelectric material induces displacement in positive and negative lattice elements which themselves induces dipole moments. This results in formation of an electric field which gives an electric potential on the electrodes. This effect is also called as generator effect [48]. The second type is the reverse or indirect piezoelectric effect, where the piezoelectric material develops a mechanical force due to the application of an electric field. This effect is called the motor effect. In the present context, the first effect, namely the generator effect has been

utilized. Piezoelectric devices are used in applications such as sensors, actuators, motors, high power and voltage source and etc. Several materials such as Lead-Zirconate-Titanate (PZT), Lead-Titanate ($PbTiO_2$), Lead-Zirconate ($PbZrO_3$) and Barium-Titanate ($BaTiO_3$) have been found to exhibit piezoelectric effect [48].

The relation between the electrical and elastic properties of piezoelectric materials [48] are given by,

$$D = d * \mathbf{T} + \varepsilon^T * E \quad , \quad 5\text{-}1$$

$$S = s^E * \mathbf{T} + d * E \quad , \quad 5\text{-}2$$

where D represents the dielectric displacement, $\mathbf{T}$ is mechanical stress, E is the electric field, S is mechanical strain, d is piezoelectric charge constant, ε^T is permittivity (for T = constant) , s^E elastic constant (E = constant).

In piezoelectric ceramic materials, the ferroelectric domains are aligned by applying a DC voltage across it. The number of domains aligned depends upon voltage, temperature and duration for which the voltage is applied on the material. This process is generally known as poling [49]. Once this process has been successful performed and when a voltage is applied across the electrodes in the poling direction, the thickness of the piezoelectric material between the electrodes increases and the thickness parallel to the electrodes decreases as shown in Figure 5-1. Similarly applying the voltage in the opposite direction will decrease the thickness of piezoelectric material between the electrodes and increase the thickness parallel to the electrodes shown in Figure 5-1. Applying a compressive force perpendicular to the electrodes or a tensile force in the direction parallel to electrodes, will generate voltage with a polarity similar to the voltage applied during poling of the material. Similarly a compressive force applied parallel to the electrodes or a tensile force applied perpendicular to the electrodes will results in a voltage generated with polarity opposite to the voltage applied during poling of the material. Applying a shear force to the piezoelectric material will also generate voltage [49].

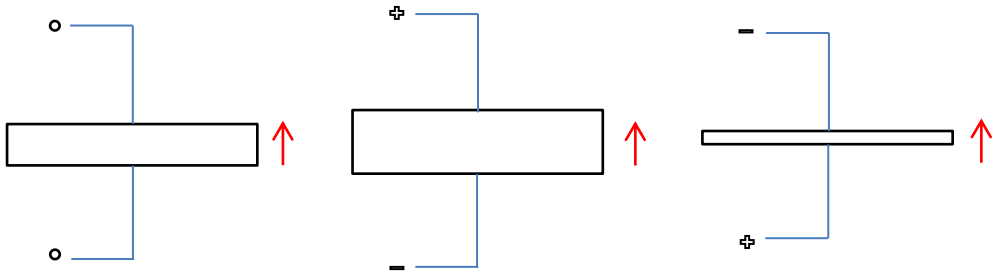

Figure 5-1 Deformation of piezoelectric elements when voltage is applied in different directions with respect to the poling direction (↑)

5.3 Piezoelectric based energy harvesting system for Solar Roadways

In order to investigate the feasibility of generating auxiliary power i.e. in addition to the solar power to be generated by Solar Roadways, the use of piezo based energy harvesting system are suggested in the present study. It is known that stresses are developed on the top cover of the solar panel due to the vehicles moving over it. Using piezoelectric elements these stresses can be harnessed to generate electricity. The electricity generated through this energy harvesting method can partly be used to overcome the inherent energy losses in the solar panels.

5.3.1 Piezoelectric elements for solar roadways

For analyzing the proposed mechanics and power output of the energy harvesting system for the solar roadways applications COMSOL Multiphysics software is used. Lead Zirconate Titanate (PZT-5A) type of piezoelectric material has been selected for the analysis. As shown in Figure 5-2, the dimensions of each piezoelectric element are chosen to be (60mm x 60mm x 10mm), these piezoelectric elements chosen for the COMSOL analysis on the manufacturers specifications, are known to generate 130V DC when a force of 1500N is applied. Typically, the voltages generated are known to vary ± 30% depending on the layout, stiffness of the plates sandwiching the PZT and etc. based on the information available from the manufactures [50]. For the present application these piezoelectric elements are placed in between the solar panel top cover and the base layer. The piezoelectric elements in COMSOL Multiphysics software are generally polarized in the z direction, which is then rotated according to the deformation of the

piezoelectric elements. The piezoelectric elements are fixed at one end, so that it can limit the piezoelectric elements from any movement due to the load applied on it. The positive and negative terminals are placed respectively in the top and bottom of the piezoelectric element. As the vehicles passes over the solar panels, load of the vehicle induces a strain on the piezoelectric elements. This strain induced electricity is used in the output power predictions. The maximum principal stress that the selected PZT-5A is subjected to for the bicycle and the motorbike loads, respectively, are 3.14Mpa and 1.4 Mpa and are lower than the tensile strength of 27.6Mpa [51] for the selected material. Hence, the PZT selected material can work under these loads without failure.

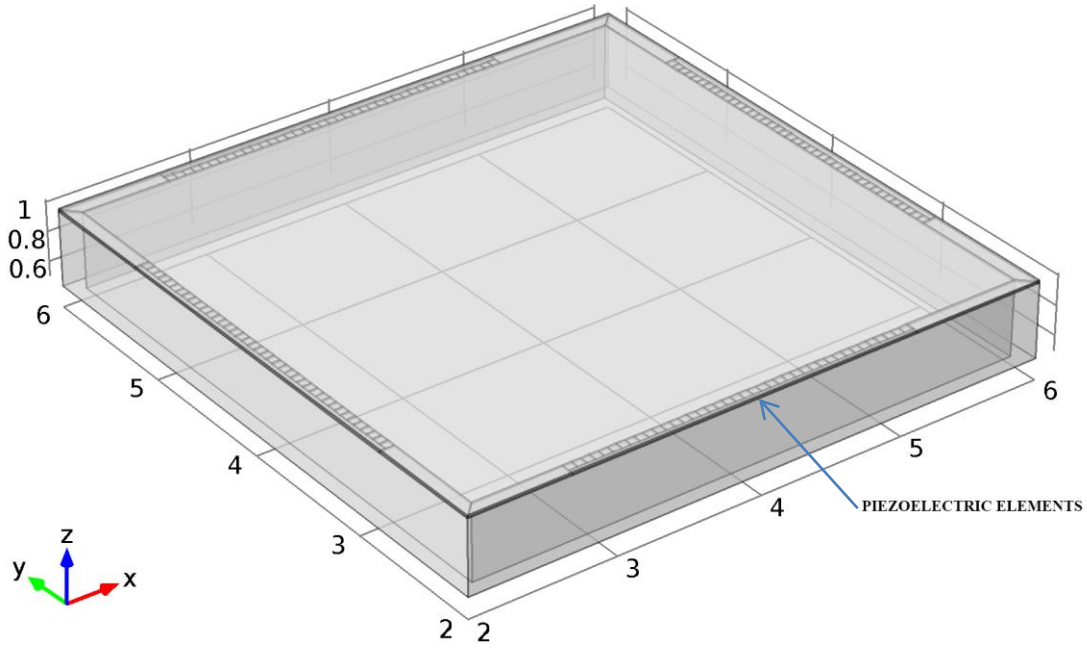

Figure 5-2 Piezoelectric elements in COMSOL model

5.3.2 Power output from the energy harvesting system

As shown in Figure 5-2 piezoelectric elements are fixed only at the inner edges of the base layer in the Solar Roadways solar panel model and at the mid portions where the strain due to the load of the vehicle over the solar panel is quite high. For the model, placements of 40 piezoelectric elements on each side of the base layer have been

assumed. Each piezoelectric element is connected to an external load of resistance 160 k ohms. Two presently viable solar roadways application cases have been evaluated for comparing with the solar power that can be derived from respective solar panels. The maximum power output from the piezoelectric element when a motorbike moves over the solar panel has been predicted to be 6W. The variation in the power output as the motorbike moves over the solar panel is shown in the Figure 5-3. This is the power output from one piezoelectric element. Due to the variation of load acting on the piezoelectric element based on its position, the power output from them also varies.

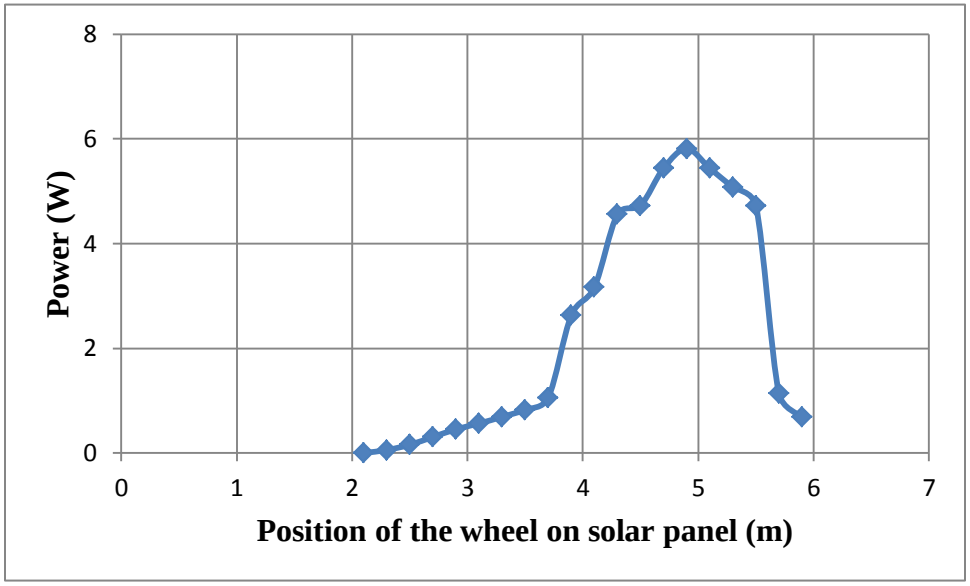

Figure 5-3 Power output from the piezoelectric element when a motorbike moves over solar panel

A solar panel modeled specifically for the bicycle path has also been analysed with the piezoelectric elements in order to ascertain the feasibility for implementations. Similar to the solar panels used in the Solar Roadways application, the solar panels for the bicycle path also have their piezoelectric elements fixed only at the inner edges of the base layer and at the mid portion as shown in Figure 5-4. For this application 12 piezoelectric elements on each side of the base layer have been considered. Each piezoelectric element is assumed to be connected to an external load of resistance 160 k ohm. The maximum power output from the piezoelectric element when a bicycle moves over the solar panel has been found to be 7.5W. The variation in the power output as the bicycle moves over

the solar panel is illustrated in Figure 5-5. Larger maximum power output from the bicycle load when compared to that from the motorbike load as depicted in Figures via Figures 5-3 and 5-5 may be attributed to the assumed larger thickness for the solar panel top cover used in the analysis for the motor bike which resulted in lower stress levels.

Further, energy produced by the solar panel with an auxiliary energy harvesting system for a bicycle lane is calculated numerically for a lane where an average of 250 bicycles / day pass through. The energy produced by the solar panel when connected to a similar external load used for the auxiliary energy harvesting system can generate approximately 1465.96kJ per day and may be subjected to an additional energy loss of 5% due to the shades caused by the bicycles moving over it. On the other hand, under similar conditions, the proposed Auxiliary energy harvesting system can produce 61.2kJ per day due to the bicycles moving over it, which is around 4.4% of energy produced by the solar panels. It may be noted that this output can be further increased if additional output due to people walking over these solar panels are also taken into account.

In the present study, for the purpose of evaluating the feasibility of auxiliary energy harvesting system developed for the solar roadways, stationary load of the vehicles over the solar panel are considered. However, to get the actual power output from these system, appropriate dynamic loads i.e. loads move over the solar panel top cover in real time have to be considered. It may be postulated that, these loads may have the capability to generate strain values that are higher than those values predicted using the roving static loads. However, the power output of piezoelectric elements due to excessive dynamic loads may also undergo fluctuation depending on the dynamic load and the vehicle speed. Hence for implementation, such an energy harvesting system may require special power conditioning for improving the quality of the power output.

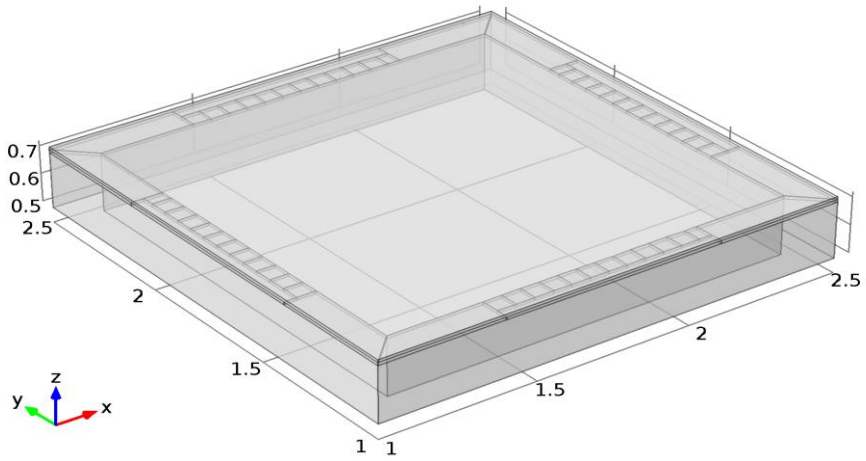

Figure 5-4 Solar panel model for bicycle path

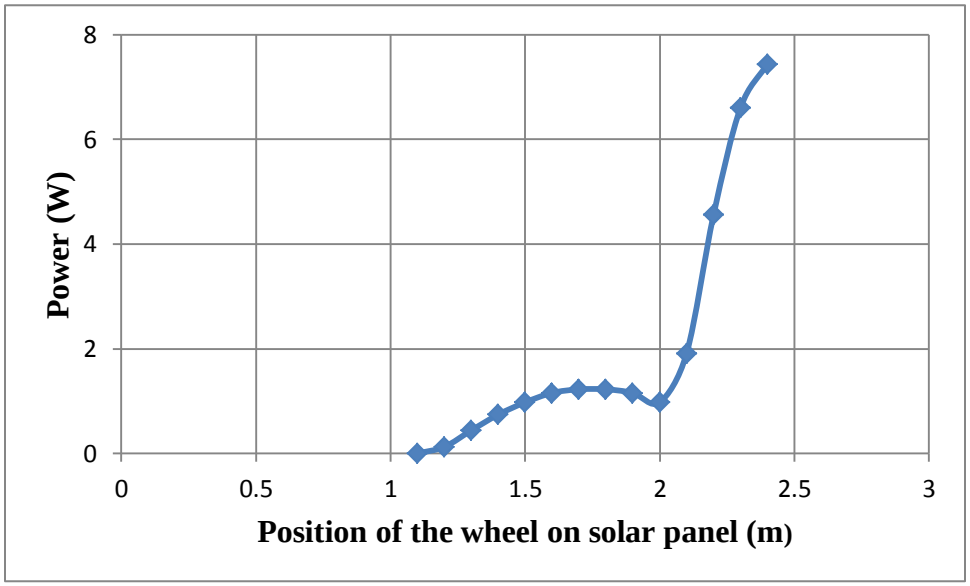

Figure 5-5 Power output from the piezoelectric element when a bicycle moves over solar panel

5.4 **Optimal placement of piezoelectric elements**

Energy harvesting is a process which captures the energy released as waste and converts them into a useful form. Thus energy harvesting process is always used to improve the efficiency of a system. Hence, optimization of the position of the energy harvesters plays an important role for improving the power output. Piezoelectric elements are used as an

energy harvester to capture the strain induced voltage caused by the vehicles moving over the solar panels. For example, this energy harvesting method can be a useful mechanism for overcoming the output losses in the solar panels due to the shadow caused by the vehicles moving over it.

5.4.1 Optimal placement based on COMSOL analysis

As shown in Figures 4-4, 4-5 and 4-7 COMSOL Multiphysics analysis of the solar panels for the Solar Roadways application demonstrated compressive stress development in the solar panel top cover as the vehicles move over it. As shown in Figure A-2, when the vehicles move over the solar panel top cover, the load of the vehicles also causes deflection on the top cover. This deflection results in increased stresses along the path of the vehicle on the solar panel top cover and at the places where the inner edge of the base layer and the solar panel top cover meets. In order to improve the efficiency of the piezo based energy harvesting process, the piezoelectric elements are placed only at the places where the stresses due to the vehicles moving over solar panel top cover are high. Based on the COMSOL Multiphysics analysis, the piezoelectric elements are placed near the inner edges of the base layer and for a length of 1.3 meters from the center line of the solar panel. The piezoelectric elements are not placed along the outer edge of the base layers and at the corners, as the stresses due to the deflection of the solar panels top cover have been found to be relatively low. The piezoelectric element arrangement for the solar roadways solar panels are shown in Figure 5-2.

5.4.2 Natural frequency analysis using COMSOL

Various modes of vibration of the selected material was found using Eigen frequency study node of the COMSOL software. As shown in Figure 5-6, for analysis purpose top cover model of size 745 mm x 675 mm x 5.6 mm was modeled. The size of the model was reduced to verify the results experimentally. So that they conform to the dimensions of the specimen used in the verification experiment. A commercially available acrylic plastic is selected as a material for the analysis. The edges of the model are considered fixed. The first few dominant modes of natural frequencies obtained from the analysis

are 16.036 Hz, 52.74 HZ, 66.77Hz, 86.66Hz and 104.43 Hz. This model is then used in the experimental analysis for placement of piezoelectric elements.

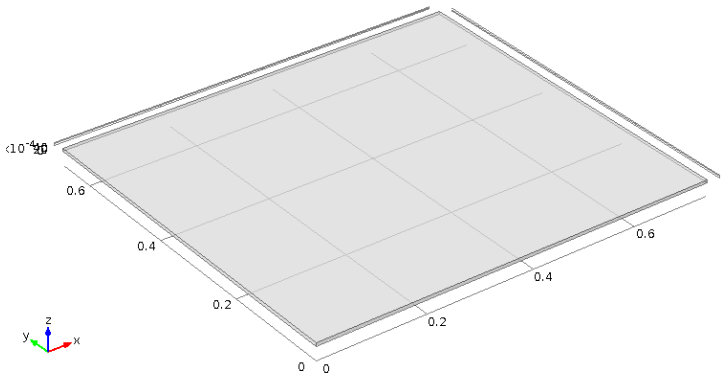

Figure 5-6 Model for natural frequency analysis using COMSOL

5.5 **Placement of piezoelectric elements via experimental analysis**

In addition to the COMSOL process developed for predicting the optimal location of the piezoelectric elements, an experimental system is developed for providing insight into the placement. The study via transient response analysis and via modal analysis is proposed. Optimal placement of the piezoelectric elements based on the results from COMSOL Multiphysics analysis was compared by simulating the similar conditions experimentally. Figure 5-7 shows the experimental setup used for the transient analysis. For simulating the condition of vehicle moving over the solar panels, a solar panel model as shown in Figure 5-8 was built with a base layer of size (745 mm x 675 mm x 63.5 mm), made of steel channels and the top cover of size (745 mm x 675 mm x 5.6 mm), made of acrylic plastic sheet. A rectangular solar panel model is considered instead of a square used in Solar Roadways system, due to the constraints in using the available structural specimens. The steel channels are attached together by clamping at corners by L shaped clamps. The acrylic plastic top cover is pinned at the corners to the base layer by means of bolts and nuts. In order to simulate the vehicles moving over the solar panel, steel balls of size one inch in diameter are rolled over the solar panel experimental model. For varying the velocity of the ball rolling over the panel, a PVC pipe has been used and its

height is varied. The vibrational displacements of the solar panel top cover surface are measured using a laser based non-contact vibration measurement system.

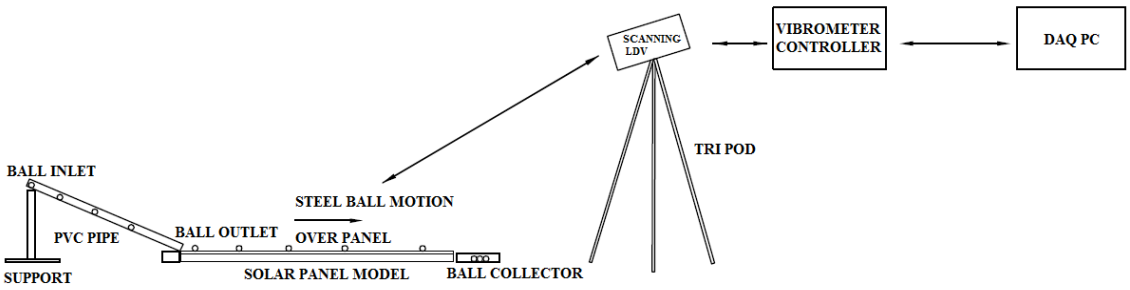

Figure 5-7 Experimental setup for optimizing the position of piezoelectric elements in auxiliary energy harvesting system

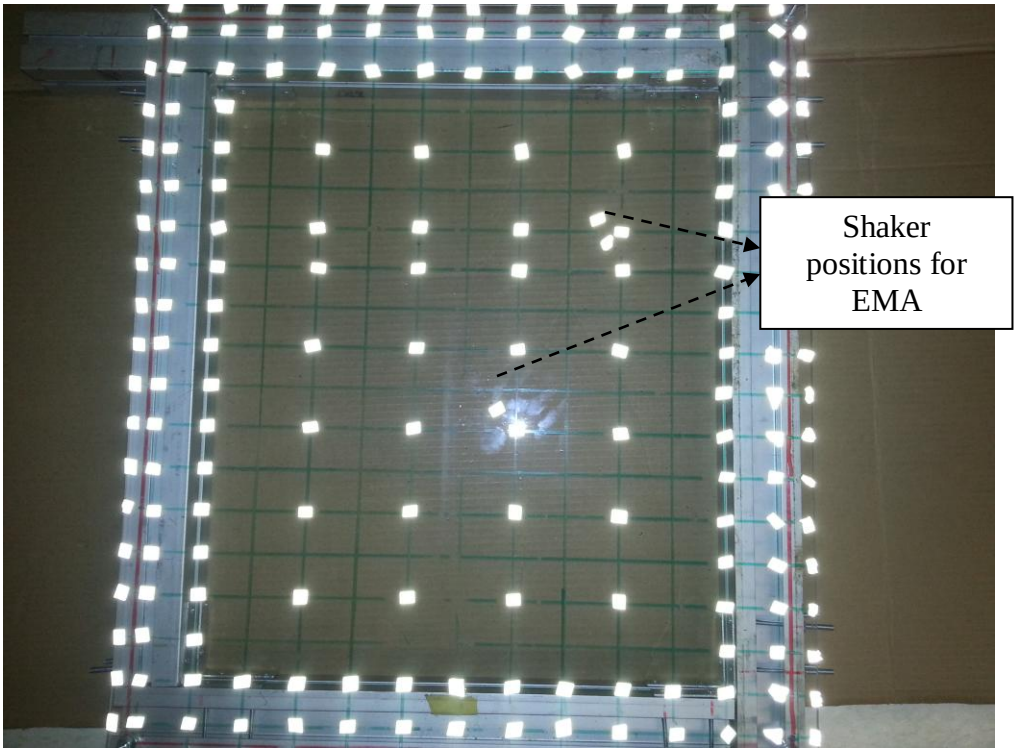

Figure 5-8 Solar panel model with scanning points marked with retro reflective tape

5.5.1 Scanning laser Doppler vibrometer system

Scanning Laser Doppler vibrometer (LDV) is a non-contact measurement tool, which can measure, visualize and analyse out of plane structural vibrations. It can directly determine the operational deflection shape (ODS) and the natural frequencies. The surface scanning feature makes the prediction of the ODS possible and the LDV system is hence able to measure over a wide range of frequency bandwidths. Polytec's PSV400 scanning LDV is used in the present experiment. It is designed to measure vibrations in both small and large structures and can support frequencies up to 24 MHz, vibration velocities up to 0.02 μm/s to 20 m/s and accelerations up to 9 million g [52]. The PSV400 scanning LDV system consists of a PSV-I-400 sensor head which includes OFV-505 vibrometer sensor, precision scanner and a video camera with auto focus. The vibrometer system also includes OFV-5000 modular vibrometer controller which processes the vibration signals and PSV-W-401 data management system from which the scanning points, acquisition mode, frequency bandwidth and all other measurement parameters are set.

5.5.2 Experimental setup for the vibrometer

For scanning purposes, equally spaced grids are marked on the solar panel model as shown in Figure 5-8. Self-adhesive retro reflective tapes are then attached to the marked grid points on the solar panel. These points act as the scan points for the scanning vibrometer. A shaker is used to vibrate the experimental structure for the purposes of experimental modal analysis (EMA) and steel balls are rolled over the solar panel model to simulate the vehicles moving over the solar panel for the transient response analysis. As shown in Figure 5-8, in the first modal analysis, the shaker is placed close to the center of the solar panel model and in the second, the shaker is placed away from the center of the solar panel model. A total number of 199 scan points have been used for the scanning vibrometer measurement and an acquisition mode of FFT has been selected. The frequency bandwidth is fixed at 400Hz measured from 2Hz to 400Hz. The details of input parameter settings used for EMA for the solar panel models are given in Appendix B1. For the transient analysis the steel balls are rolled through a pipe from a certain height, so that the rolling velocity of the steel balls within the panel domain can be

approximated to be constant. In this experiment a total of 84 scan points have been used for the scanning vibrometer measurements. An acquisition mode of FFT and frequency bandwidth of 1 kHz measured from 1.25Hz to 1 kHz has been chosen. The input parameter information used for the moving load analysis of the solar panel models is given in Appendix B2.

5.5.3 Results from the scanning vibrometer

For the modal analysis measurements from all the 199 scanning points are utilized by the scanning vibrometer. Vibration at each point is measured 10 times and their average values are determined. From the two modal analyses experiment performed the shaker positions have been found not make significant variations in the results. The vibration velocity for entire bandwidth of measured frequency in the modal analysis of the solar panel model is shown in Figure 5-9. The entire bandwidth consists of all first few dominant modes. The results from the scanning vibrometer showed that the maximum vibration velocities are present at the center and along the edges closer to the center line of the panel. The dominant modes of frequencies obtained from this software have been found to have 14Hz, 52Hz, 66Hz, 88Hz and 102Hz as natural frequencies. These values matched closely with the values obtained from the COMSOL analysis. Matching of natural frequencies proved the ability of model developed in COMSOL to predict the results closely with real conditions.

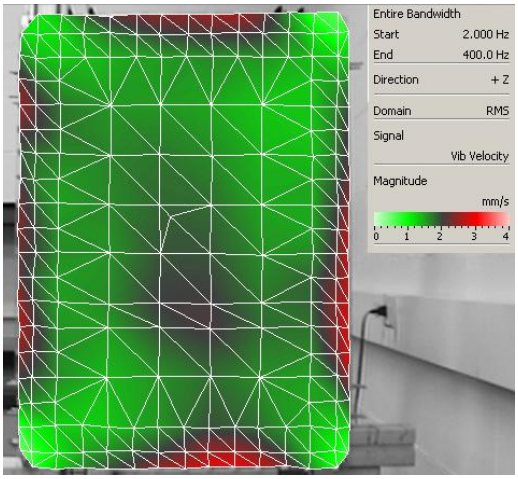

Figure **5-9** Vibration velocity for entire bandwidth (Experimental modal analysis)

For the moving load analysis of the solar panel model, steel balls are rolled over the panel. In the moving load analysis, the numbers of scanning points for the scanning vibrometer are reduced to 84 points. The vibration velocity for entire the bandwidth of measured frequency in the modal analysis of the solar panel model is shown in Figure 5-10. The results from the scanning vibrometer showed that the maximum vibration velocities are present at the center and along the edges closer to the center line of the panel. But the maximum vibrations are also present near the corners of the panel, which has not been predicted by the COMSOL Multiphysics analysis. These variations in the results can be mainly attributed to improper fixing of the solar panel top cover with the base layer.

As a part of this study, a procedure for optimizing the location of piezoelectric elements is formalized using both COMSOL and experimental methods for future analysis. It is envisaged that this system can be employed to predict the output power from an auxiliary energy harvesting system, when materials suitable for the Solar Roadways system become available. Power generation ratio i.e. solar and piezoelectric can also be validated using these methods prior to implementation.

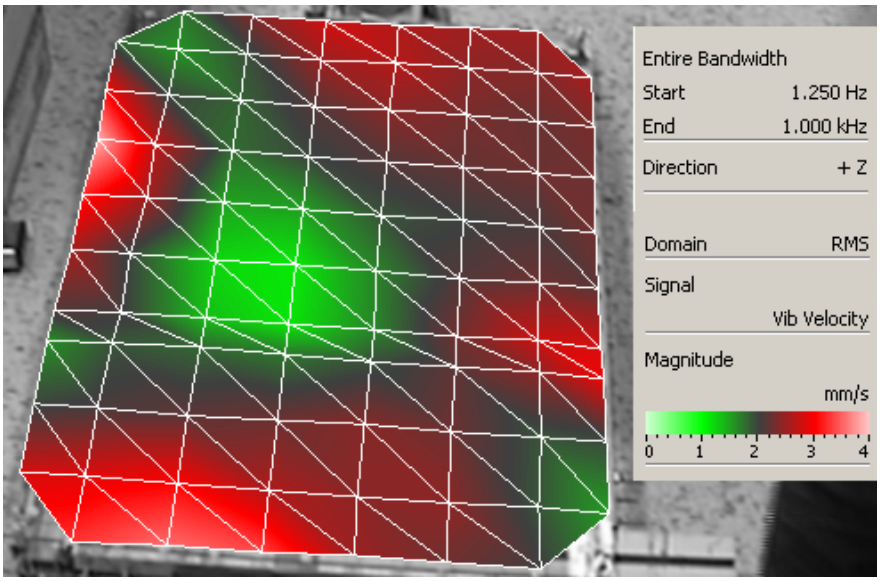

Figure 5-10 Vibration velocity for entire bandwidth (Moving load analysis)

5.6 **Summary**

In this chapter a method using both COMSOL and vibration experiments are developed to optimize positions of the piezoelectric elements for use in the auxiliary energy harvesting system for the Solar Roadways. The power output from these piezoelectric elements can be used to overcome the energy losses in the solar panels of the Solar Roadways system. A solar panel with piezoelectric elements was modelled specifically to be used in the cycle path.

Chapter 6

6 Conclusion

6.1 Summary of Research

This thesis describes work directed to study various potential outcomes that can be derived from implementation of the Solar Roadways system and difficulties in implementing such a system. A detailed feasibility study for the Solar Roadways system in Canada has been conducted by calculating the total amount of electricity by covering all the existing roads in Canada with solar panels. By covering all the roads in Canada with the solar panels, the electricity generated from these solar panel have been shown to be sufficient to supply power to 32 cities similar in size to Toronto for a year. Thus, implementation of Solar Roadways system can result in possible reduction in the use of non-renewable energy resources as well as in the pollution caused while generating electricity.

In a typical Solar Roadways system, vehicles move over the solar panels and these vehicles can cause shades over the solar panels. Effect of these fast moving shades on the output of the solar panels and various other losses that are involved in the Solar Roadways application has been studied. It was shown that the fast moving shades over the solar panels cause rapid fluctuations in the power output from the solar panels. The total area covered by the shades and the total drop in the solar irradiance value falling over the solar panel are the major parameters which control the amount of energy lost in the system. The speed with which the vehicle moves over the solar panels determines the period for which there is a reduction in the output from the solar panels. In a typical solar panel, several other losses due to effects such as temperature, panel mismatch, tilt angle and inverter efficiency are present and these losses can add up to decrease the overall efficiency of the solar panel in producing electricity. Hence, Monte Carlo uncertainty analysis is used to predict how the solar panels behave when the solar irradiance value are varied from the standard test condition value of 1000 W/m^2. When the solar irradiance value reaches higher than the standard test condition value, the output from the solar panel continued to be around its maximum output and did not undergo significant

increase. However, when the solar irradiance values are lower than the standard test condition value, the output from the solar panel reduced drastically.

One of the major hurdles in implementing the Solar Roadways system is to determine a material for the top cover of the solar panels, which can allow maximum amount of sunlight falling over them to reach the solar cells while possessing sufficient strength to take on the load of the vehicles moving over the solar panels. Using COMSOL Multiphysics software, the load carrying capacity of the existing materials has been analyzed. When the acrylic plastic material is selected for solar panel top cover, it resulted in failing to take the load of a typical truck and a car moving over it. When the thickness of the solar panel is increased to 25.4mm, the material has been demonstrated to take on the load of a motorbike moving over it. It is also found that the acrylic plastic is able to take on the load of a bicycle moving over the solar panel. Based on the predictions, a solar panel for a bicycle lane is modeled with the same acrylic plastic as solar panel top cover.

An energy harvesting system has been suggested using piezoelectric elements, which can absorb the strain produced in the solar panel top layer and produce electricity. The efficiency of the energy harvesting system is improved by optimizing the physical locations of the piezoelectric elements, so that the proposed elements can absorb maximum strain energy from the solar panel top cover. COMSOL Multiphysics software has been employed for optimizing the position of the piezoelectric elements. The results from the COMSOL Multiphysics have been compared with the results obtained via experiments that simulate similar conditions. The methodologies developed in the present thesis using COMSOL and vibration experiments are envisaged to play an important role in the predictions of optimal positions for the piezoelectric elements and for estimating the solar/harvester power ratio before implementing the systems under real conditions. Further, in order to aid immediate implementation, a solar panel with piezoelectric elements has been modelled specifically to be used as part of a bicycle path.

6.2 **Thesis contributions**

The contributions of this thesis centre primarily on quantifying the challenges involved in the implementation of Solar Roadways, analysing the typical extreme conditions the solar panels and the associated structures are subjected to. The computational tools COMSOL Multiphysics and the PSpice software have been effectively employed for the numerical predictions together with suitable experimental validations. These contributions can be summarized as follows:

- A detailed study on the feasibility of implementing the Solar Roadways system in Canada by covering total available road surfaces in Canada with solar panels demonstrated that the electricity generated from these solar panels are sufficient to supply power to 32 cities similar in size to Toronto for a year.
- A methodology to study the effects of fast moving shades on the output of the solar panels has been developed using PSPICE and their outcomes are validated via experiments.
- Using COMSOL Multiphysics software, the load carrying capacity of the existing materials to be used as panel cover is analyzed and this methodology is envisaged to aid future studies on the characteristics of future materials to be developed for the Solar Roadways application.
- An energy harvesting method utilizing piezoelectric elements is proposed to harness the strain caused by the vehicles moving over the solar panel and this system can be used to overcome various losses in the solar panels for solar roadways application. A procedure for optimizing locations of piezoelectric elements, for the proposed energy harvesting system, and has been formalized using both COMSOL and experimental methods for future analysis.
- With the present commercially available materials, a solar panel for the bicycle lane is proposed and its feasibility is tested using COMSOL Multiphysics. This analysis is envisaged to aid the implementation of such a system in the near future.

6.3 **Recommendations for future research**

Possible extensions to, and expansions upon, the research described in this thesis are:

- This thesis demonstrated numerically the possible use of piezo-based energy harvesting and the prediction of optimal locations. Experimental verification of piezo-based energy harvesting system on a typical solar panel can now be performed and the results shall be verified.

- For the implementation of Solar Roadways system, further research is required in the development of a new material for the solar panel top cover which can take on the load and give sufficient traction for the moving vehicles and allow maximum sunlight to reach the solar cells. The desirable material properties for the Solar Roadways solar panel top cover have been identified in this thesis.

- With the development of new materials for the solar panel top cover, along with the stationary load of the vehicle over the solar panels, response to dynamic loads resulting from the vehicles also have to be analysed using COMSOL. Such a study is expected to give more accurate predictions of the load carrying capacity as well as the energy available via the piezo-based energy harvesting system. In particular, these predictions can give a better insight into the failure due to fatigue.

- It has been demonstrated in the thesis that materials that are commercially available at present when used as the panel top cover can withstand the load of a typical bicycle moving over the solar panel. Hence, both solar as well as piezo-based energy harvesting systems can be implemented in the immediate future for such a system.

Bibliography

[1] "Solar Roadways," [Online]. Available: http://solarroadways.com/intro.shtml.

[2] "Thermal Power," Ontario Power Generation, 2012. [Online]. Available: http://www.opg.com/power/thermal/. [Accessed 07 08 2012].

[3] James Gibbons, "OPG Coal Plants are Ontario's Pollution Giants," Ontario Clean Air Alliance, 01 02 2007. [Online]. Available: http://www.cleanairalliance.org/resource/opgiant.pdf. [Accessed 07 08 2012].

[4] Ben Gorman, "AltE," [Online]. Available: http://www.altestore.com/howto/Solar-Electric-Power/Design-Components/Electrical-Characteristics-of-Solar-Panels-PV-Modules/a87/. [Accessed 03 07 2012].

[5] Engin Karatepe, Mutlu Boztepe and Metin Colak "Development of a Suitable Model for Characterizing Photovoltaic Arrays with Shaded Solar Cells," *Solar Energy 81*, pp. 997-992 2007.

[6] Achim Woyte, Johan Nijis and Ronnie Belmans "Partial Shadowing of Photovoltaic Arrays with Different System Configurations: Literature Review and Field Test Results," *Solar Energy 74*, pp. 219-233, 2003.

[7] M.C. Alonso-Garcia, J.M. Ruiz and W. Heermann "Computer Simulation of Shading Effects in Photovoltaic Arrays," *Renewable Energy 31,* p. 1986–1993, 2006.

[8] L. Cortez, J.I. Cortez, A. Adorno, GA. Muñoz-Hernandez and E. Cortez "Study of the Effects of Random Changes of Solar Radiation on Energy Production in a Photovoltaic Solar Module," *Canadian Journal on Electrical and Electronics Engineering*, pp. 79-93, 2010.

[9] Ramaprabha Ramabadran, "Effect of Shading on Series and Parallel Connected Solar PV Modules," *Modern Applied Science*, pp. 32-41, 2009.

[10] A. Ibrahim, "Effect of Shadow and Dust on the Performance of Silicon Solar Cell," *Journal of Basic and Applied Scientific Research*, pp. 222-230, 2011.

[11] David Biello, "Driving on Glass Inventor Hopes to Lay Down Solar Roads," 29 10 2009. [Online]. Available: http://www.scientificamerican.com/article.cfm?id=driving-on-glass-solar-roads. [Accessed 14 08 2012].

[12] "Energy Harvesting," [Online]. Available: http://www.iop.org/resources/energy/materials/page_50300.html. [Accessed 15 08 2012].

[13] "Can House Music Solve Energy Crisis," 10 09 2008. [Online]. Available: http://science.howstuffworks.com/environmental/green-science/house-music-energy-crisis1.htm. [Accessed 30 07 2012].

[14] "Tokyo Train Station Testing Power-Generating Floor," 04 12 2008. [Online]. Available: http://cleantechnica.com/2008/12/04/tokyo-train-station-testing-power-generating-floor/. [Accessed 30 07 2012].

[15] "Road - Weigh In Motion," [Online]. Available: http://www.innowattech.co.il/slnWim.aspx. [Accessed 30 07 2012].

[16] "Estimation of the Representative Annualized Capital and Maintenance Costs of Roads by Functional Class," Applied Research Associates, Inc., 2008.

[17] "Ontario's Municipal Roads," (ORC), Ontaio roads coalition, 2003.

[18] "Road Rehabilitation Energy Reduction Guide for Canadian Road Builders," Canadian Industry Program for Energy Conservation c/o Natural Resources Canada, 2005.

[19] J. Papic, “The Windsor Square," 25 04 2011. [Online]. Available: http://www.windsorsquare.ca/?p=15128. [Accessed 03 07 2012].

[20] "Windsor 250," 25 04 2011. [Online]. Available: http://www.unconqueredsun.com/userfiles/file/Windsor%20250P%20Module%20Specs.pdf. [Accessed 03 07 2012].

[21] "Wikipedia," 27 06 2012. [Online]. Available: http://en.wikipedia.org/wiki/Insolation. [Accessed 03 07 2012].

[22] "Natural resources Canada," 21 03 2012. [Online]. Available: http://pv.nrcan.gc.ca. [Accessed 03 07 2012].

[23] "The Power to Live Green," Toronto City Council, Toronto, 2009.

[24] A. Ubisse and A. Sebitosi, "A New Topology to Mitigate the Effect of Shading for Small Photovoltaic Installations in Rural Sub-Saharan Africa," *Energy Conversion and Management 50,* pp. 1797-1801, 2009.

[25] "PSpice," [Online]. Available: http://en.wikipedia.org/wiki/PSpice. [Accessed 13 07 2012].

[26] Luis Castaner and Santiago Silvestre, Modelling Photovoltaic Systems Using PSpice, John Wiley & Sons Ltd, 2002.

[27] Christiana Honsberg and Stuart Bowden "pveducation," [Online]. Available: http://www.pveducation.org. [Accessed 05 07 2012].

[28] "Kyocera," [Online]. Available: http://www.kyocerasolar.com/. [Accessed 07 07 2012].

[29] "Provincial Highways Traffic Volume (AADT only) 2008," Ontario Ministry of Transportation, 2008.

[30] A.M.AL- Sabouchi, "Effect of Ambient Temperature on the Demanded Energy of Solar Cells at Different Inclinations," *Renewable Energy, Vol. 14,* pp. 149-155, 1998.

[31] "United Stated Renewable Energy Association," [Online]. Available: http://www.usrea.org/documents/Solar-Module.pdf. [Accessed 09 07 2012].

[32] "Wikipedia," [Online]. Available: http://en.wikipedia.org/wiki/Self-cleaning_glass. [Accessed 09 07 2012].

[33] Arbi Gharakhani Siraki and Pragasen Pillay, "Study of Optimum Tilt Angles for Solar Panels in Different Latitudes for Urban Applications," *Solar energy 86,* pp. 1920-1928, 2012.

[34] "Heliostats," 14 11 2010. [Online]. Available: http://www.heliostats.org/2010/11/cosine-loss.html. [Accessed 09 07 2012].

[35] "Performance of Solar Power Plants in India," Central Electricity Regulatory Commission, New Delhi, 2011.

[36] Saiful Islam, Achim Woyte, Ronnie Belmans and Johan Nijs, "Undersizing inverters for grid connection - What is the optimum?," *PV in Europe location:Rome, Italy,* pp. 780-783, 2002.

[37] "Ontario Renewable Energy Cooperative Inc.," 2010. [Online]. Available: http://ottawarenewableenergycoop.ca. [Accessed 10 07 2012].

[38] OrCAD PSpice A/D Reference Guide, OrCAD, 1999.

[39] COMSOL Inc., [Online]. Available: http://www.comsol.com/products/multiphysics/. [Accessed 15 07 2012].

[40] "Physical Properties of Acrylic Sheet," [Online]. Available: http://www.builditsolar.com/References/Glazing/physicalpropertiesAcrylic.pdf. [Accessed 06 09 2012].

[41] Standard Specifications for Highway Bridges, American Association of State Highway and Transportation Officials, Inc.

[42] "Attenuation Coefficient," [Online]. Available: http://en.wikipedia.org/wiki/Attenuation_coefficient. [Accessed 18 07 2012].

[43] "Mini Copper," [Online]. Available: http://en.wikipedia.org/wiki/Mini. [Accessed 21 07 2012].

[44] "2012 FZ8," Yamaha, 2012. [Online]. Available: http://www.yamaha-motor.com/sport/products/modelspecs/652/0/specs.aspx. [Accessed 21 07 2012].

[45] Denise Brehm, "Civil Engineers Find Savings Where the Rubber Meets the Road," 23 05 2012. [Online]. Available: http://web.mit.edu/newsoffice/2012/pavement-savings-tires-0523.html. [Accessed 23 07 2012].

[46] "PV Glass," Topray Solar, [Online]. Available: http://www.topraysolar.com/products_3.php. [Accessed 24 07 2012].

[47] "Bike Lanes," 2012. [Online]. Available: http://www.london.ca/d.aspx?s=/Transportation/Bike_Lanes.htm. [Accessed 24 07 2012].

[48] "Piezoelectric effect," PICeramic, [Online]. Available: http://www.piceramic.com/profile.php. [Accessed 30 07 2012].

[49] James R. Phillips, "Piezoelectric Technology Primer," New Mexico, 2008.

[50] "Piezo Ceramic Plate Energy Harvesting," STEINER & MARTINS, INC., [Online]. Available: http://www.steminc.com/. [Accessed 22 08 2012].

[51] "Typical Properties,"Morgan Technical Ceramics, [Online]. Available: http://www.morganelectroceramics.com/resources/piezo-ceramic-tutorials/typical-properties/. [Accessed 21 10 2012].

[52] "PSV-400 Scanning Vibrometer," POLYTEC Inc., [Online]. Available: http://www.polytec.com/fileadmin/user_uploads/Products/Vibrometers/PSV-400/Documents/OM_DS_PSV-400_2011_05_E.pdf. [Accessed 27 08 2012].

Appendices

Appendix A Maximum von Mises stress and displacement for various cases studied in the COMSOL analysis

Figures from COMSOL Multiphysics analysis for different cases studied to analyze the load carrying capability of the selected commercially available material to be used as a top cover of the Solar Roadways solar panel are given below. Acrylic plastic sheet with thickness 15mm and 25.4mm were analyzed for the load of car and motorbike moving over it. Maximum von Mises stress and displacement due to the applied load are shown below.

A-1 Load of a car over the solar panel top cover with a thickness of 15mm

The maximum von Mises stress, displacement and the location at which they occur due to the load of a car over the solar panel are given below:

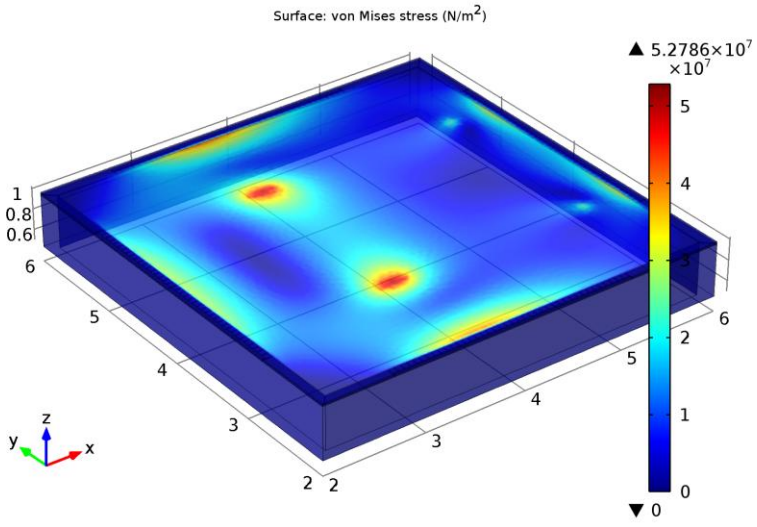

Figure A-1 Maximum von Mises stress for load of a car with a top cover thickness 15 mm (at front wheel location of 5.5m)

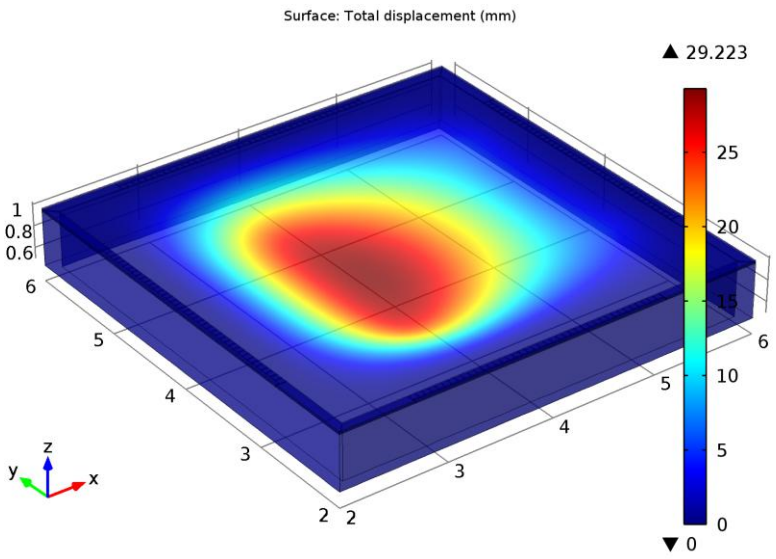

Figure A-2 Maximum displacements for a load of a car with a top cover thickness 15 mm (at front wheel location of 5.5m)

A-2 Load of a car over the solar panel top cover with a thickness of 25.4mm

The maximum von Mises stress, displacement and the location at which they occur due to the load of a car over the solar panel are given below:

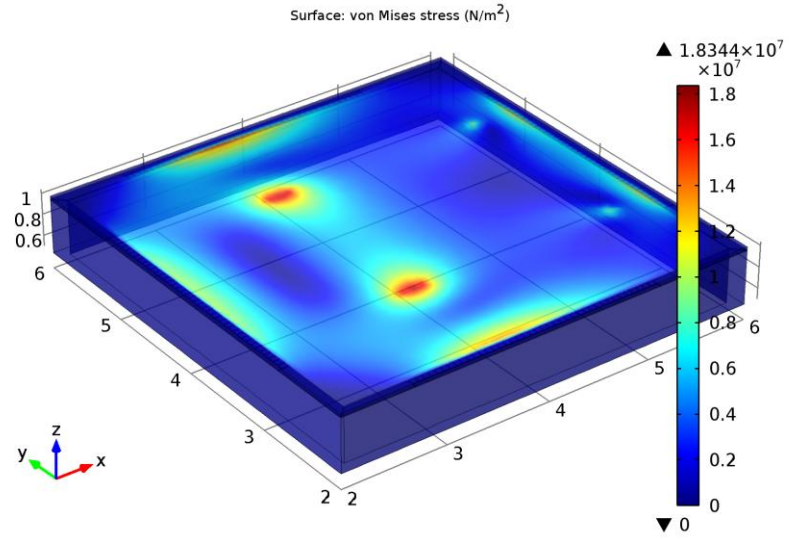

Figure A-3 Maximum von Mises stress for load of a car with a top cover thickness 25.4 mm (at front wheel location of 5.5m)

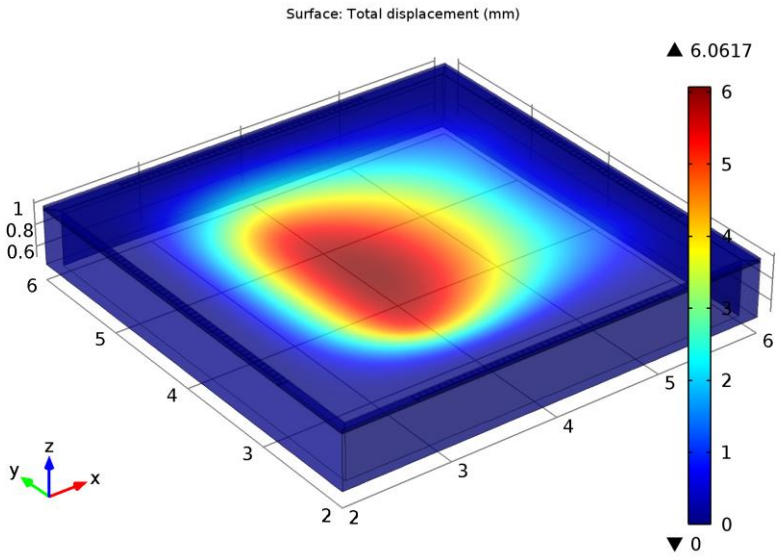

Figure A-4 Maximum displacements for load of a car with a top cover thickness 25.4 mm (at front wheel location of 5.5m)

A-3 Load of a motorbike over the solar panel top cover with a thickness of 15mm

The maximum von Mises stress, displacement and the location at which they occur due to the load of a motorbike over the solar panel are given below:

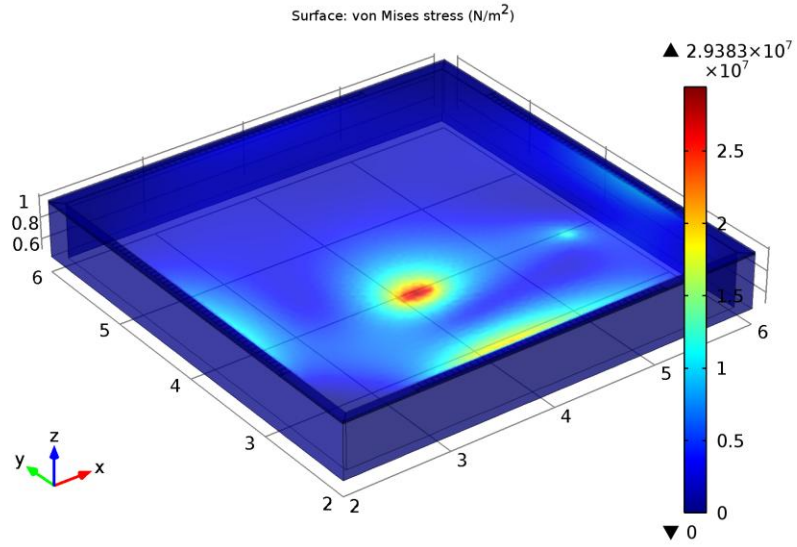

Figure A-5 Maximum von Mises stress for load of a motorbike with a top cover thickness 15 mm (at front wheel location of 5m)

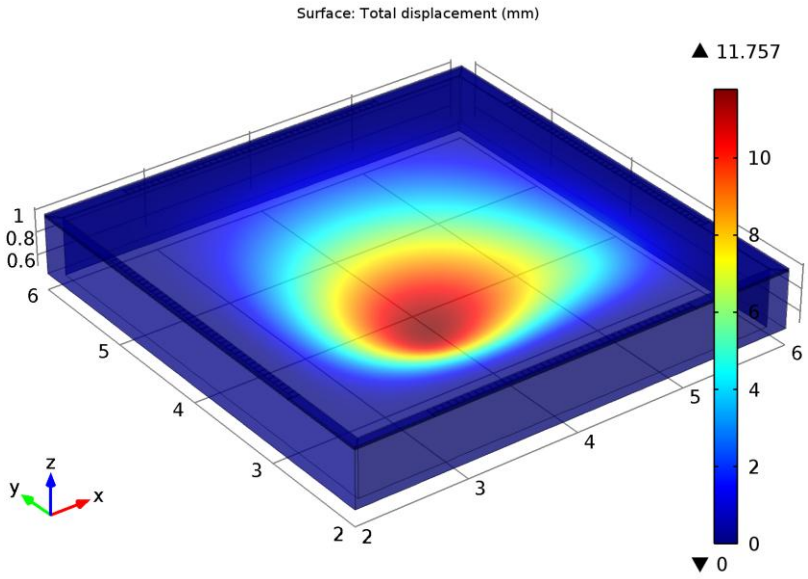

Figure A-6 Maximum displacements for load of a motorbike with a top cover thickness 15 mm (at front wheel location of 5m)

A-4 Load of a motorbike over the solar panel top cover with a thickness of 25.4mm

The maximum von Mises stress, displacement and the location at which they occur due to the load of a motorbike over the solar panel are given below:

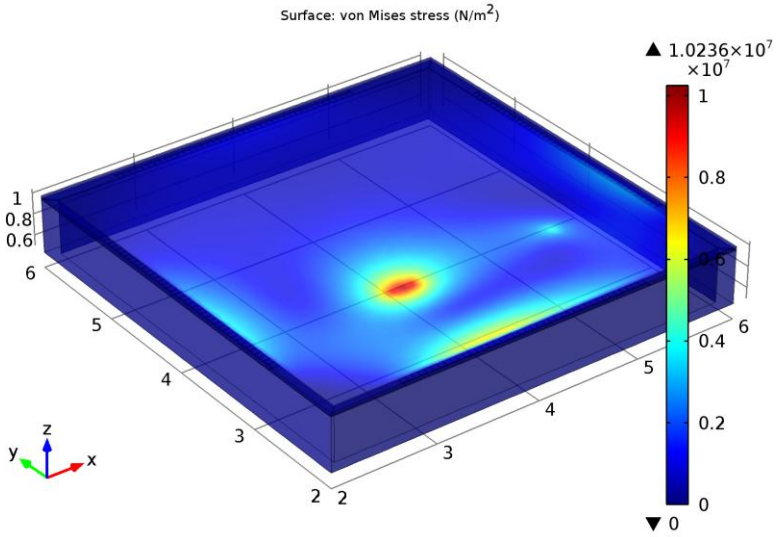

Figure A-7 Maximum von Mises stress for load of a motorbike with a top cover thickness 25.4 mm (at front wheel location of 5m)

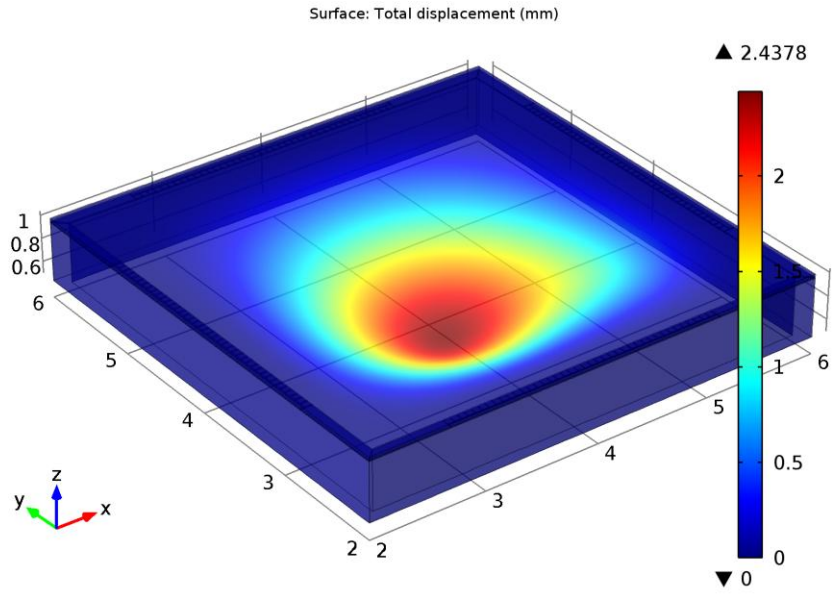

Figure A-8 Maximum displacements for load of a motorbike on solar panel with a top cover thickness 25.4 mm (at front wheel location of 5m)

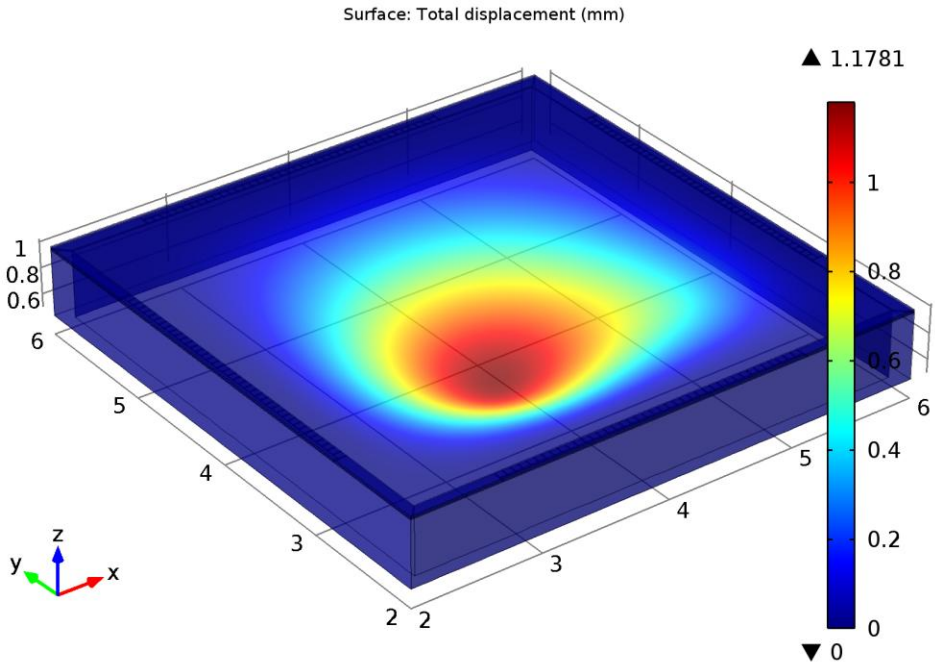

Figure A-9 Maximum displacement for load of a motorbike on solar panel top cover (Increased Young's Modulus of the top cover material)

A-5 Summary of results from COMSOL analysis

All the results from COMSOL analysis for various load cases and a solar panel top cover thickness of 10mm are given below and the values shaded with yellow marks the maximum von Misses stress and maximum displacement.

Table A-1 Maximum von Mises stress and displacement of vehicles used for COMSOL analysis

X position of wheel(s) (m)	Truck (Load due to rear wheels)		Car (Load due to all wheels)		Motorbike (Load due to all wheels)	
	Maximum von Mises stress (N/m2) x 10^9	Maximum Displacement (m)	Maximum von Mises stress (N/m2) x 10^7	Maximum Displacement (m)	Maximum von Mises stress (N/m2) x 10^7	Maximum Displacement (m)
2.1	0.752	0.0002	4.023	0.0000	0.940	0.0000
2.2	0.986	0.0184	5.280	0.0010	1.740	0.0003
2.3	1.090	0.0614	5.850	0.0033	1.950	0.0011
2.4	1.100	0.1207	5.900	0.0065	1.980	0.0021
2.5	1.270	0.1911	6.790	0.0102	2.305	0.0032
2.6	1.380	0.2694	7.360	0.0144	2.318	0.0044
2.7	1.500	0.3531	8.010	0.0189	2.720	0.0056
2.8	1.570	0.4408	8.420	0.0236	2.885	0.0068
2.9	1.700	0.5313	9.080	0.0285	2.875	0.0080
3	1.640	0.6226	8.750	0.0333	2.982	0.0090
3.1	1.590	0.7100	8.540	0.0380	2.778	0.0099
3.2	1.620	0.7916	8.650	0.0424	2.920	0.0108
3.3	1.740	0.8661	9.300	0.0464	2.944	0.0115
3.4	1.710	0.9324	9.160	0.0499	3.060	0.0122
3.5	1.688	0.9895	9.030	0.0530	3.049	0.0127
3.6	1.820	1.0368	9.770	0.0555	3.309	0.0133
3.7	1.778	1.0739	9.500	0.0575	3.211	0.0136
3.8	1.780	1.1008	9.550	0.0589	3.230	0.0141
3.9	1.679	1.1168	8.992	0.0598	4.262	0.0161
4	1.720	1.1222	9.203	0.0601	4.199	0.0159
4.1	1.781	1.1168	9.530	0.0598	4.013	0.0168
4.2	1.750	1.1007	9.397	0.0592	3.196	0.0159
4.3	1.780	1.0739	9.530	0.0605	4.303	0.0202
4.4	1.800	1.0366	9.633	0.0608	4.542	0.0214
4.5	1.740	0.9894	9.324	0.0580	4.530	0.0205
4.6	1.700	0.9323	9.098	0.0611	4.703	0.0243
4.7	1.635	0.8660	8.740	0.0523	4.690	0.0236
4.8	1.680	0.7915	8.950	0.0612	4.580	0.0268

4.9	1.645	0.7098	8.730	0.0617	4.799	0.0276
5	1.630	0.6224	8.640	0.0570	6.549	0.0395
5.1	1.699	0.5316	8.970	0.0584	4.940	0.0276
5.2	1.500	0.4407	8.355	0.0603	3.110	0.0157
5.3	1.513	0.3530	8.450	0.0672	4.748	0.0287
5.4	1.440	0.2693	8.577	0.0684	4.984	0.0281
5.5	1.302	0.1910	11.700	0.0982	4.749	0.0278
5.6	1.118	0.1207	9.090	0.0697	4.840	0.0273
5.7	1.061	0.0614	11.700	0.0354	3.058	0.0136
5.8	1.010	0.0183	8.967	0.0702	2.949	0.0131
5.9	1.390	0.0002	8.970	0.0697	2.920	0.0126

Table A-2 von Mises stress and displacement of bicycle used for COMSOL analysis

X position of the one wheel (m)	**Bicycle (Load due to all wheels)**	
	Maximum von Mises stress (N/m2) x 10^7	**Maximum Displacement (mm)**
1.1	0.931	0.001
1.2	5.564	0.080
1.3	0.813	0.234
1.4	0.922	0.400
1.5	0.903	0.545
1.6	1.030	0.647
1.7	0.963	0.703
1.8	1.050	0.704
1.9	1.030	0.649
2	0.949	0.545
2.1	1.590	0.425
2.2	1.520	0.508
2.3	1.680	0.958
2.4	1.750	1.403
2.5	1.350	0.817
2.6	1.550	0.971
2.7	2.030	2.059
2.8	2.060	1.988
2.9	1.990	1.767
3	1.420	0.817
3.1	1.270	0.600
3.2	1.480	0.467
3.3	0.948	0.120
3.4	1.610	0.002

Appendix B Input parameter information sheet of the scanning LDV

For experimentally optimizing the position of piezoelectric elements used in the Solar Roadways energy harvesting system, scanning vibrometer system was used. The input parameter information sheets of the scanning vibrometer system for the modal and the moving load analysis of the solar panel model are given below:

B-1 Input parameter information sheet of the scanning vibrometer system for modal analysis of solar panel model

```
 Scan Points

 Total:                      199
 Not measured:               0              0.0 %
 Valid:                      0              0.0 %
 Optimal:                    199            100.0 %
 Over range:                 0              0.0 %
 Invalidated:                0              0.0 %
 Disabled:                   0              0.0 %
 Not reachable:              0              0.0 %
 Hidden:                     0              0.0 %
 ------------------------------------------------------------------
-----
 Scanning Head:              PSV-I-400 LR  (OFV-505)
 Junction Box:               PSV-E-401-M2-20
 Acquisition Board:          Spectrum MI3025
 ------------------------------------------------------------------
-----
 General

 Acquisition Mode:           FFT
 Averaging:                  Complex
 Averaging count:            10
 PCA (MIMO):                 Not active
 Cosine correction X:        Active
 Cosine correction Y:        Active
 ------------------------------------------------------------------
-----
 Frequency

 Bandwidth:                  400 Hz
 Bandwidth from:             2 Hz
 Bandwidth to:               400 Hz
 ------------------------------------------------------------------
-----
 Sampling

 FFT Lines:                  200
```

```
Sample frequency:            1.024 kHz
Sample time:                 500 ms
Resolution:                  2 Hz
-------------------------------------------------------------
Trigger

Source:                      Off
-------------------------------------------------------------
Channel Vibrometer (connected to Vibrometer 1)

Direction:                   +Z
Range:                       10 V
Coupling:                    DC
Impedance:                   1 MOhm
Quantity:                    Velocity
Calibration factor:          10e-3 (m/s)/V
Signal Delay:                5.85e-6 s
Filter Type:                 Band Pass
Quality:                     Very High
Cut-off Frequency 1:         10 Hz
Cut-off Frequency 2:         400 Hz
Int/Diff Quantity:           Velocity
Window:                      Hanning
Signal Enhancement:          Active

Channel Reference 1

Reference point index:       0
Direction:                   +Z
Range:                       200 mV
Coupling:                    DC
Impedance:                   1 MOhm
Quantity:                    Force
Calibration factor:          88.96 N/V
Signal Delay:                0 s
Filter Type:                 Band Pass
Quality:                     Very High
Cut-off Frequency 1:         10 Hz
Cut-off Frequency 2:         400 Hz
Int/Diff Quantity:           Force
Window:                      Hanning
Signal Enhancement:          Not active
-------------------------------------------------------------
Signal Enhancement

Speckle Tracking:            Active
Mode:                        Fast
-------------------------------------------------------------
Vibrometer 1

Type:                        OFV-5000
Tracking filter:             Off
```

```
Velocity output

Range:                          10 mm/s/V
Low pass filter:                5 kHz
High pass filter:               Off
-----------------------------------------------------------------
Function Generator 1

Type:                           MI 60xx
Signal:                         White Noise
Amplitude:                      1 V
Offset:                         0 V

-----------------------------------------------------------------
```

B-2 Input parameter information sheet of the scanning vibrometer system for moving load analysis of solar panel model

```
Scan Points

Total:                          84
Not measured:                   0               0.0 %
Valid:                          0               0.0 %
Optimal:                        84              100.0 %
Over range:                     0               0.0 %
Invalidated:                    0               0.0 %
Disabled:                       0               0.0 %
Not reachable:                  0               0.0 %
Hidden:                         0               0.0 %
-----------------------------------------------------------------
Scanning Head:                  PSV-I-400 LR  (OFV-505)
Junction Box:                   PSV-E-401-M2-20
Acquisition Board:              Spectrum MI3025
-----------------------------------------------------------------
General

Acquisition Mode:               FFT
Averaging:                      Off
PCA (MIMO):                     Not active
Cosine correction X:            Active
Cosine correction Y:            Active
-----------------------------------------------------------------
Frequency

Bandwidth:                      1 kHz
Bandwidth from:                 1.25 Hz
Bandwidth to:                   1 kHz
-----------------------------------------------------------------
Sampling
```

```
FFT Lines:                    800
Sample frequency:             2.56 kHz
Sample time:                  800 ms
Resolution:                   1.25 Hz
------------------------------------------------------------------
Trigger

Source:                       Off
------------------------------------------------------------------
Channel Vibrometer (connected to Vibrometer 1)

Direction:                    +Z
Range:                        10 V
Coupling:                     DC
Impedance:                    1 MOhm
Quantity:                     Velocity
Calibration factor:           100e-3 (m/s)/V
Signal Delay:                 4.21e-6 s
Filter Type:                  Band Pass
Quality:                      Very High
Cut-off Frequency 1:          5 Hz
Cut-off Frequency 2:          400 Hz
Int/Diff Quantity:            Velocity
Window:                       Rectangle
Signal Enhancement:           Active

Channel Reference 1

Reference point index:        0
Direction:                    +Z
Range:                        10 V
Coupling:                     DC
Impedance:                    1 MOhm
Quantity:                     Force
Calibration factor:           88.96 N/V
Signal Delay:                 0 s
Filter Type:                  Band Pass
Quality:                      Very High
Cut-off Frequency 1:          5 Hz
Cut-off Frequency 2:          400 Hz
Int/Diff Quantity:            Force
Window:                       Rectangle
Signal Enhancement:           Not active
------------------------------------------------------------------
Signal Enhancement

Speckle Tracking:             Active
Mode:                         Fast
------------------------------------------------------------------
Vibrometer 1

Type:                         OFV-5000
```

Tracking filter:	Off
Velocity output	
Range:	100 mm/s/V
Low pass filter:	5 kHz
High pass filter:	Off

Curriculum Vitae

Name:	Rajesh Kanna Selvaraju
Education and Degrees:	The University of Western Ontario London, Ontario, Canada 2010-2012 MESc. Mechanical and Materials Engineering. SASTRA University Thanjavur, Tamil Nadu, India 2003-2007 BE Mechanical Engineering
Scholarships:	Western Graduate research Scholarship The University of Western Ontario 2011-2012
Related Work Experience	Teaching Assistant The University of Western Ontario 2011-2012 Mechanical Engineer Alpan Consulting Engineers Pvt. Ltd. 2007-2008 Graduate Engineering Trainee BHEL Piping Center 2008-2009